DEVELOPMENT OF SCREEN PRINTED ELECTRODES BASED ON NANOMATERIAL MODIFIED PAPER FOR BIOMEDICAL APPLICATION

to be submitted as Major Project in partial fulfillment of the requirement for the degree of

M. Tech. (Biomedical Engineering)

Submitted by

Anas Saifi

(Roll No. 2K15/BME/02)

Delhi Technological University

Under the supervision of

Prof. Bansi D. Malhotra

Department of Biotechnology

Delhi Technological University, Delhi 110042, India

DECLARATION

I, **Anas Saifi**, hereby declare that the dissertation entitled **'Development of screen printed electrodes based on nanomaterial modified paper for biomedical application '** submitted is in partial fulfillment of the requirement for the award of the degree of Master of Technology in Biomedical Engineering, Delhi Technological University. It is a record of original and independent research work done by me under the supervision and guidance of **Prof. Bansi. D. Malhotra**, Department of Biotechnology, Delhi Technological University, Delhi. The information and data enclosed in the dissertation is original and has not formed the basis of the award of any Degree/Diploma/Fellowship or other similar title to any candidate of the University/Institution.

Date:

Anas Saifi
Roll No.: 2K15/BME/02
M. Tech. (Biomedical Engineering)
Department of Biotechnology
Delhi Technological University
Shahbad Daulatpur,
Main Bawana Road, Delhi 110042, INDIA

Delhi Technological University

Certificate

This is to certify that the dissertation entitled '**Development of screen printed electrodes based on nanomaterial modified paper for biomedical application**' submitted by Anas Saifi (2K15/BME/02) is in the partial fulfillment of the requirements for the reward of the degree of Master of Technology, Delhi Technological University, Delhi, is an authentic record of the candidate's own work carried out by her under my guidance. The information and data enclosed in this thesis is original and has not been submitted elsewhere for honoring of any other degree.

Prof. D. Kumar
(Head & Co-Supervisor)
Department of Biotechnology
Delhi Technological University

Prof. Bansi D. Malhotra
(Project Supervisor)
Department of Biotechnology
Delhi Technological University

Acknowledgement

I wish to express my profound sense of gratitude to my mentor Prof. Bansi D. Malhotra, Department of Biotechnology, Delhi Technological University for his valuable guidance, much sought-after suggestions and encouragement throughout these investigations. I heartily thank Prof. D. Kumar, Head, Department of Biotechnology, Delhi Technological University, for his kind support and help in providing all facilities in a timely manner.

I am highly indebted to Dr Saurabh kumar, Dr Saurabh Shrivastava, Ms. Shine Augustine and Dr Suveen Kumar (Research Scholars) whose guidance and constant supervision helped me decide on my project work and complete it in a timely manner.

I thank all the faculty members of Department of Biotechnology, Delhi Technological University for providing me with valuable suggestions and all necessary facilities required to complete this project work. I also thank Mr. Chhail Bihari Singh, Mr. Jitender Kumar and all other non-teaching staff of Department of Biotechnology, Delhi Technological University for aiding me in finding requirements for the project work.

I thank my fellow colleagues Ratan Kumar, Rahul Kandpal, Tarun Narayan and Ashish Kalkal for assisting me when in need and encouraging me to carry out this work.

Lastly, this report would not have been possible if not for the patience and encouragement of my family. I thank my parents for their support throughout the framing of this report.

Anas Saifi

2K15/BME/02

List of Abbreviations

CA	Contact angle
CE	Counter Electrode
CV	Cyclic Voltammetry
EIS	Electrochemical Impedence Spectroscopy
FTIR	Fourier Transform Infrared Spectroscopy
GO	Graphene Oxide
GOx	Glucose Oxidase
HCl	Hydrochloric acid
H_2O_2	Hydrogen peroxide
H_2SO_4	Sulphuric acid
H_3PO_4	Phosphoric acid
$K_2S_2O_8$	Potassium Persulphate
KMnO4	Potassium permanganate
LOC	Lab-on-chip
NaOH	Sodium hydroxide
PBS	Phosphate buffered Saline
PET	Polyethylene Tetraphthalate
POC	Point-of-care
PTFE	Polytetrafluoroethylene
RE	Reference electrode
rGO	Reduced graphene Oxide
SEM	Scanning electron microscopy
SPE	Screen printed electrodes
UV-vis-NIR	Ultra-Violet visible Near Infrared Spectroscopy
WE	Working electrode
XRD	X-ray diffraction

List of Figures

Table of Content

DEVELOPMENT OF SCREEN PRINTED ELECTRODES BASED ON NANOMATERIAL MODIFIED PAPER FOR BIOMEDICAL APPLICATION

Anas Saifi
Delhi Technological University, New Delhi.
E-mail ID: saifianas23@gmail.com

Abstract

In this work, a new screen printed paper-based electrochemical sensor is developed as a low-cost and disposable point-of-care device for glucose detection. A cellulose paper disk is modified with biocomposite of reduced graphene oxide and glucose oxidase (rGO-GOx). Further, rGO-GOx modified paper electrode has been used as an electrochemical cell for storage of $[Fe(CN)6]^{3-/4-}$ ions as mediator and phosphate buffer. The electrochemical signals are recorded by adding glucose to the modified paper disc which is placed on top of a SPE. This biosensor exhibited a linear range of 50 to 500 mg/dl glucose (R^2 = 0.99), with a remarkable sensitivity of 0.331 µAdl/mg and a limit of detection of 0.12 mg/dl. This minaturized electrochemical setup is simple, lightweight, portable, low cost and is disposable.

1) Introduction

The electrochemical biosensors have been found to play a major role for desired analytical and clinical applications due to their high S/N ratio, high sensitivity, portability and faster analysis. An additional advantage of electrochemical detection is the effortlessness of the instrument bringing about low power requirements to utilize in-field. [1, 2] The electrochemical system comprises of three electrodes such as working, reference and a counter electrode. This three electrode system is dipped into an electrochemical cell containing a buffer/electrolyte solution to obtain an electrochemical signal. For the fabrication of electrochemical biosensor ITO, glassy carbon, and gold electrodes are conventionally used as a working electrode, platinum as an auxiliary electrode, Ag/AgCl as the reference electrode and a glass vial is used as an electrochemical cell. To address the need of on-site analysis, it was necessary to remove such traditional complex, rigid, and expensive assemblies. [3] With global technological and economic advancements, the focus has shifted on reducing the manufacturing costs and miniaturisation of the device. Today cheap and affordable approaches are being exploited for the achievement of the same. [4]

Screen printed electrodes (SPE) enable miniaturisation of the device since all the 3 electrodes are printed on a few cm^2 area of a substrate area making it inexpensive and simple. It offers precise control over electrode dimensions, excellent uniformity, maintains an adequate level of reproducibility and capable of undergoing mass production. [5-8] It has reformed the field due to their potential to bridge the gap between laboratory experiments with in-field usage. [9, 10] For direct analysis of a sample in its natural condition, SPEs have enabled the production of advanced sensors which can be incorporated in portable systems. [11] Further miniaturisation of device

offers several advantages such as the small volume of sample required, faster analysis time, increased reliability and repeatability. [12-14]

Among the different transduction techniques for SPEs, the most attracted method of detection was electrochemical detection due to its low cost and faster analysis. [15] SPEs based electrochemical sensors have plenty of scope to improve their performance by integrating with Whatman filter paper. [16, 17] The 3D hierarchical porous structure of Whatman paper enables it to act as an efficient reagent storing material, owing to absorption. The interconnected porosity provides faster access to ionic species and the electrode surfaces. [18-21] Additionally, it can be modified with nanomaterials making it convenient to introduce electrochemical properties, biomolecule immobilization, reagent storage capacity, stability and shelf life. In this context, reduced graphene oxide (rGO) has recently wakened much interest for the fabrication of paper modified electrochemical sensor. [22-24] This is because of their excellent electrochemical properties, large surface area, solution processability, mechanical flexibility and strong adsorption over paper surface. Its abundant chemical groups facilitate charge transfer as well as provide a site for biomolecule immoblization. [25, 26] Moreover, small band gaps and excellent conductivity of rGO are favourable for conduction of electrons from the biomolecules and promote the electron transfer between electrostatic species and electrodes. [27] Thus rGO modified papers can be utilised as reagent storing electrochemical cells having enhanced electron transfer rate and improved biomolecule loading, sensitivity and stability.

Here, we report the results of studies relating to the development of a paper modified screen printed electrode for glucose detection. This miniaturized electrochemical electrode is simple, lightweight, portable, low-cost and is disposable. Doping of paper with rGO and it result in improved electrochemical characteristics of the screen-printed electrode. This modified paper disc

screen printed electrode has been used as an immobilization matrix for glucose oxidase. Since the enzymes do not have long-term stability, the highly porous microstructure which contains fine fibres provides a suitable support for enzyme immobilization through simple adsorption mechanism i.e. the cellulose paper is reported as a pre-storage matrix for the reagents.

2) Literature & Review

2.1) Diabetes

Diabetes is a medical condition in which the body does not sufficiently produce the quantity or quality of insulin expected to maintain a normal blood glucose. The normal blood glucose concentration of healthy person is in a range, i.e. 70-180 mg/dl. Insulin is a hormone that facilitates glucose to enter the body's cells that can be utilized for energy. Unmonitored diabetes can lead to consequences over time like heart failure, kidney failure, blindness and peripheral neuropathy related to poor circulation, limb pain, gangrene and subsequent amputation henceforth long-term damage, dysfunction and failure of various organs are some of the final results of diabetes mellitus.

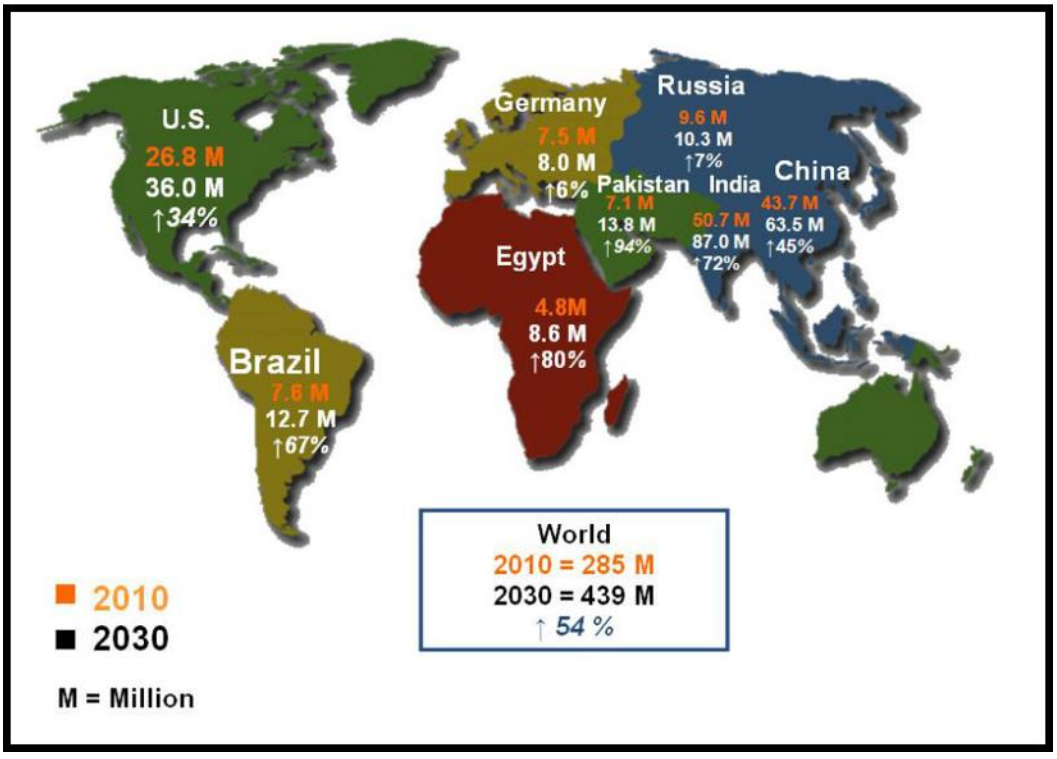

Fig 2.1: Latest stats on Diabetes from World Health Organization.

From recent survey report of World Health Organization (WHO), it is observed that 220 million individuals worldwide are suffering from the metabolic disorder i.e. Diabetes Mellitus. In

the year 2012, diabetes is the direct cause of an estimated 1.5 million deaths, and it is said that number will probably increase to 366 million by the year 2030. [28] This increasing prevalence while including the developing nations too is represented below in the World Diabetes Map issued by the WHO on 2010.

Benchmarking 80%, maximum deaths due to diabetes occurred in low and middle-income countries, and the highest number is in India, China and USA. It was considered that a disease like diabetes must resulted from an overindulgent lifestyle and economic changes of the people belonging to the urbanized nations. However, in recent years, there were several reports published revealing high prevalence in communities of developing nations also in ethnic minorities of industrialized countries like Native Americans, Pacific Islanders and migrant Asian Indians. [29]

The majority of people who have diabetes are in the age group of 45 to 64 years. While over a decade surprisingly there has been an increase in the cases of diabetes in teenagers. [30] It is also observed globally that diabetes among adults ageing above 18 has risen from 4.7% (1980) to 8.5% (2014). [31]

Diabetes may present with characteristic symptoms such as thirst, loss of weight, blurring of vision and polyuria. While in its most serious forms i.e. ketoacidosis state may create and lead to coma, stupor and might be death if untreated. Often symptoms are not serious or may be absent and consequently hyperglycaemia of adequate degree to cause pathological changes might be available for a while before the diagnosis is made.

2.1.1) Types of diabetes

In a diabetic patient, either the pancreas secretes limited little or no insulin (type 1 diabetes), or the cells do not respond appropriately to the insulin that is produced (type 2 diabetes). In particular, "*Type 1 diabetes*", i.e. Insulin Dependent Diabetes Mellitus (IDDM) is described by loss of the

insulin-producing beta cells leading to the deficiency of insulin. Mostly type 1 diabetes has an autoimmune origin and it directly affects young adults or children, and sometimes it is also referred to as juvenile diabetes.

Other than above, "*Type 2 diabetes*" i.e. Non-Insulin-Dependent Diabetes Mellitus (NIDDM), is described by insulin resistance which might be consolidated with relatively lower insulin secretion. Insulin resistance relates to a loss of efficiency of insulin action which causes a reduction in glucose from the blood to the cells. It is often associated with overindulgent lifestyle and obesity considered as the most common diabetes almost 90% of cases which mostly affects adult people. [32]

2.1.2) Diabetes-Related Complications

A failure of the regulatory system to counter glucose causes Blood Glucose Levels (BGL) to surpass the euglycaemic range, Moreover Hypoglycemia and hyperglycemia may prompt to short and long-term complications, respectively.

Hyperglycemia has no instant damaging consequence on the organism, however, if this state occurs frequently and hold on for a long time, it would lead to several complications. Hyperglycemia includes both, micro and macrovascular complications which involve small and large blood vessels respectively [33]. To prevent the onset of these complications, different diabetes therapies are pursed to keep BGL within the range. This can be accomplished with physical activity, management of diet, and use of appropriate medications

The failure of body's regulatory system to counter glucose and unawareness towards therapy could cause, principally during physical activity and sleep hours, significantly more dangerous and unfavourable effect like hypoglycemia.

Hypoglycemia affects the brain, given its consistent glucose demand. Subsequently, when glucose levels fall, brain functions declines due to which people may lose cognitive abilities and in the some cases patients might go into hypoglycemic coma. Hypoglycemia has mainly short-term effects [34] and can be classified according to the level of awareness:

- ***Mild hypoglycemia*** in which blood glucose levels between 55 and 70 mg/dL is described by palpitations, trembling, excessive sweating, extreme hunger, cold and visual paleness, due to blood redirection to the vital organs and minimization of the peripheral blood circulation. In this situation, a small amount of carbohydrate diet could restore normal glucose levels.
- ***Moderate hypoglycemia*** is within the range of 55 and 40 mg/dL. The symptoms of hypoglycemia include irritability, blurred vision, mood changes, confusion, drowsiness and weakness since it affects the central nervous system.
- ***Severe hypoglycemia*** comes under 40 mg/dL and is described by coma, loss of consciousness, hypothermia and convulsions. If this condition is hold on for long time could cause irreversible heart problems and brain damages, or even death. In such cases, intravenous dextrose or glucagon injection is required.

2.2) Conventional techniques

The Diabetes Care and Complications Trial (DCCT) suggest that monitoring of blood glucose and insulin levels on a regular basis may avoid many of the long-term complications related to diabetes. [35]

The broadly categorized conventional methods for blood glucose measurement are:

1. Urine analysis
2. Blood analysis

3. Non-invasive analysis

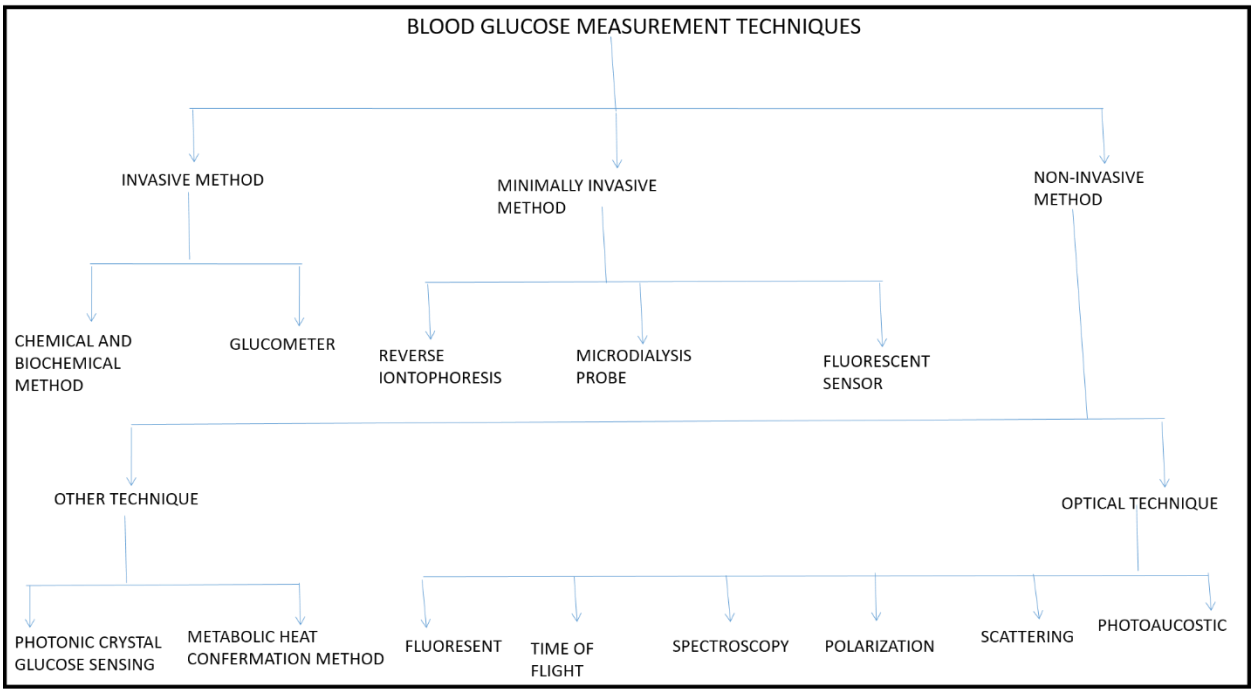

Fig 2.2: Glucose measurement techniques.

2.2.1) Urine analysis

Earlier strategies like testing of urine by patient themselves with the help of by Benedict's copper reagent possessed practical problems like the requirement of heat for the colour to develop. Compton and Treneer at Ames in 1945, came up with a modified copper reagent tablet "clinitest" containing all the necessary reagents giving a nearly ideal solution to the previous problem. [36]

A small volume of urine and the tablet are taken in a tube for biochemical reaction to produce adequate heat which causes the mixture to boil. Oxidation and reduction of glucose (in urine) and blue cupric sulphate respectively, trigger a course of chemical reactions causing a series of colour changes from blue to green to yellow and finally orange. Semi-quantitative results could be acquired by visual examination of the formation of colour with a predefined chart. A similar test based on the use of reagent tablets detects ketones in human urine around the 50s.

Advantages

(i) The method is easy to operate

(ii) low-cost

(iii) faster analysis.

Disadvantages

(i) lower precision.

(ii) Non-reliable.

(iii) A skilled person is required to carry out the test.

(iv) Physiological conditions like pH, temperature etc may differ the results.

2.2.2) Blood analysis

Most commonly glucose meters are based on the oxidation of glucose to gluconolactone, where glucose oxidase (GOx) is being used as a catalyst. Some use glucose dehydrogenase (GDH) as a catalyst instead, as it is more sensitive than GOx but is also more susceptible to other possible interfering reactions.[36]

Calorimetric reactions based on the first-generation devices are still in use today as quantitative glucose measurement devices. The characteristic blue colour is of an oxidised benzidine derivative which is also included in the kit. The oxidation is carried out by the produced hydrogen peroxide in the reaction. The strips should be developed after precise intervals and also the metre required to be frequently calibrated. These factors proved to be major disadvantages of this kit. Modern day glucometer is based on electrochemical methods. Capillaries of the test strip suck up the reproducible amount of blood, of which glucose is allowed to react with GOx/GDH at the enzyme electrode. Mediator reagents, such as a ferricyanide ion, a ferrocene derivatives are used for reoxidization of the enzyme. However, the mediator is reoxidised by reaction at the

electrode surface which generates an electrical current. The total electrical current which passes through the electrode surface is directly proportional to the glucose level present in the blood. [36]

Advantages

(i) More reliable method.

(ii) The method gives high precision and accuracy.

(iii)No skilled person is required, can be operated by the patient himself.

Disadvantages

(i) It is an Invasive method.

(ii) Low-cost.

(iii) Short shelf life, and variation of results because of the physiological conditions.

(iv) Colorimeter utilized for the analysis requires calibration every time.

2.2.3) Research & Development of non-invasive methods

Medical domain generally uses non-invasive optical sensors for the diagnosis via providing information from blood & tissues as a part of the specimen. Some methods which are developed for non-invasive blood glucose measurement are summoned below: [37], [38]

- **Raman spectroscopy** mainly works on laser light to generate oscillation and rotation in molecules. While subsequent emission of scattered light altered by this molecule vibration depends on the glucose concentration. [39]
- **Infrared spectroscopy** deals with absorption and scattering of Infrared light; procedure started when these infrared lights concentrated on human tissues and interacts with biological components within the tissues. Absorption of energy in the infrared region results as soon the interaction produces molecular vibration. This vibrational absorption depict to wavelength in the order of 4000-400 cm^{-1}. [39]

- **Fluorescent spectroscopy**: works principally when the light of some specific frequencies irradiated on human skin, it generates fluorescence which can be utiliized for blood glucose detection. [39]
- **Thermal spectroscopy** is a technique based on the theoretical concept of infrared radiation emiitting from the human body which is also proportional to glucose absorption. [39], [40]
- **The photoacoustic technology** excites the body fluid with the help of laser, while its acoustic response is proportional to blood glucose concentration. [37], [38]

Presently glucose measurement procedure starts with pricking a finger to obtain 50 µl blood drop. This blood drop is placed over a test strip which is glucose sensitive. The blood sample is then analyzed by an optical glucometer which gives an analytical reading of glucose.

2.3) Enzyme

In 1877, a German physiologist Wilhem kuhne coined the term 'enzyme' (en=in, zyme=yeast). [41] These are proteins which act as catalysts in the conversion of substrates into their respective products i.e. they are capable enough to increase reaction rates of order 10^6 to 10^{18} using specific substrates.

Enzymatic reactions are usually fast and by many folds than their un-catalysed counterparts. Their functionality is increased by the fact that they require non-protein cofactors. An enzyme is described by its charge, structure and hydrophilic/hydrophobic nature. The specificity of an enzyme can be classified into four categories, namely: group, absolute, linkage and stereochemical specificity. Group specificity enables the enzyme to catalyse reactions which involves a substrate with a specific functional group while in an absolute specificity the enzyme catalyze only a single reaction. In Linkage specificity the enzymes catalyzes the reactions

involving specific chemical bond and in stereochemical specificity, the enzyme acts on a specific stereoisomer directed by the chirality of the binding sites of enzyme [42].

2.3.1) Enzyme specificity

The interactions between enzymes and substrates can broadly be understood by two key concepts: (i) lock-and-key hypothesis and (ii) induced fit hypothesis. The lock-and-key hypothesis, fig 2.3 (a), denotes that only a specific substrate can accurately fit the enzyme's active site. The induced fit hypothesis which is proposed by Koshland fig 2.3 (b), states that a three-dimensional change in enzyme can occur by a specific substrate, and thus aligns enzyme with the substrate which leads to the formation of a enzyme-substrate complex and generates a product. [43]

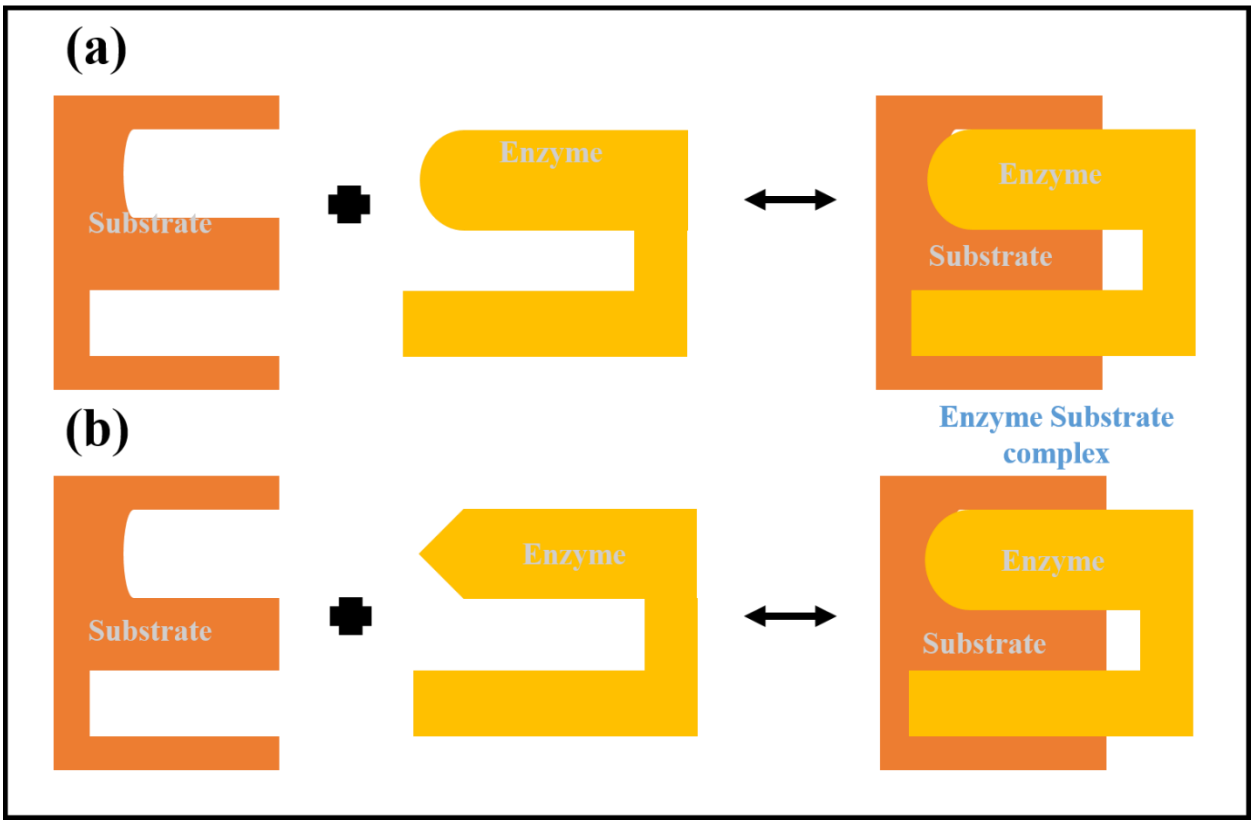

Fig 2.3: Schematic diagram of the a) lock and key model and (b) induced fit hypothesis.

2.3.2) <u>Enzyme kinetics</u>

The most important parameter of enzyme kinetics is the initial rate (V_0) in the enzymatic reaction which corresponds to a known substrate concentration. (Fig. 2.4). Michaelis and Menten in 1913 put forward a mechanism to better understand how the initial rate of enzyme-catalyzed reactions depends on the concentration, which is now known as the Michaelis-Menten equation i.e.

$$V_0 = V_{max} \frac{[S]}{K_m + [S]} \qquad 2.1)$$

where V_{max} = the maximum rate of the reaction at saturating substrate concentrations, [S] = concentration of substrate, K_m = Michaelis constant, defined as:

$$K_m = \frac{k_{-1} + k_2}{k_1} \qquad 2.2)$$

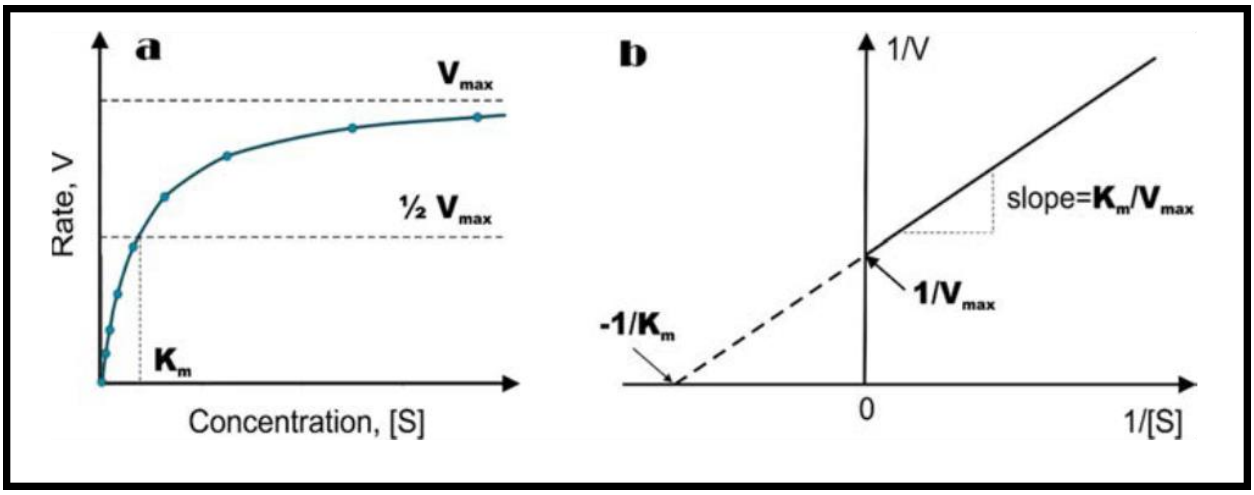

Fig. 2.4 a) The initial rate of the enzyme catalyzed reaction *vs.* concentration. b) LB plot.

Equation (2.1) is one of the principle equations of enzyme kinetics.

$$V_0 = \frac{1}{2} V_{max} \rightarrow K_m = [S] \qquad 2.3)$$

where V_{max} and K_m can be determined from Fig. 2.4 (a). Though these can be more conveniently determined by the Lineweaver and Burk equation:

$$\frac{1}{V_0} = \frac{K_m}{V_{max}\,[S]} + \frac{1}{V_{max}} \qquad 2.4)$$

In Fig. 2.4 (b) V_{max} and K_m represent the intercept and slope of the straight line respectively. K_m is highly specific and changes with both the change in enzymes as well as substrate. K_m depends on source of enzyme, ionic strength, temperature, pH and other physiological conditions.

V_{max} is the maximum rate of reaction, when all enzyme molecules are present in the enzyme-substrate complex state:

$$V_{max} = k_2\,[E_0] \qquad 2.5)$$

Given a known initial concentration of the enzyme $[E_0]$ and V_{max}, values of k_2 can easily be determined (eq. 2.1, 2.2 and 2.5), where k_2 = ***'turnover number'*** which is also called $\boldsymbol{k_{cat}}$ refers the catalytic constant. It is the maximum number of substrate molecules which are converted to product per catalytic site in an unit time. [44]

Glucose oxidase is one of the most commonly used enzymes in biosensors. The reaction scheme for glucose oxidase (GOx) is given below in eq (2.6)

$$O_2 + \text{glucose} \rightarrow H_2O_2 + \text{gluconic acid} \qquad 2.6)$$

The structure of this GOx constitutes of two identical subunits and one FAD coenzyme molecule. The molecular weight of GOx is 186,000 g/mole and a size of 70 Å x 55 Å x 80 Å.

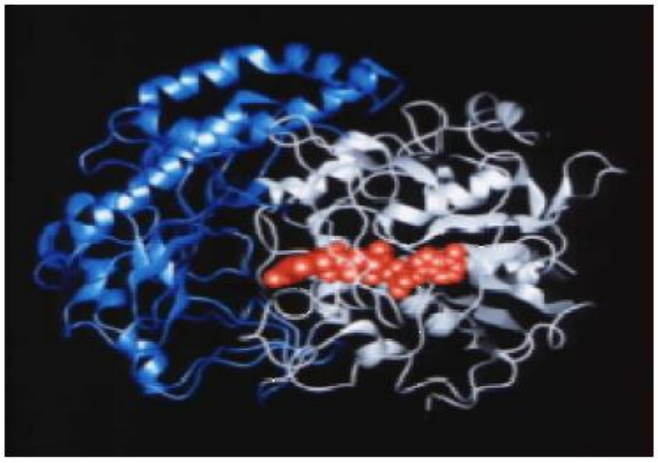

Fig 2.5: The structure of Glucose Oxidase.

The red space fill indicates FAD coenzyme molecule which is present in the active site of GOx (fig. 2.5), which is connected tightly but not covalently bound to the enzyme. FAD has a reversible electrochemical activity making it an efficient cofactor. Two hydrogen atoms are needed to convert FAD (fully oxidized state) to $FADH_2$ (fully reduced state) (fig 2.6).

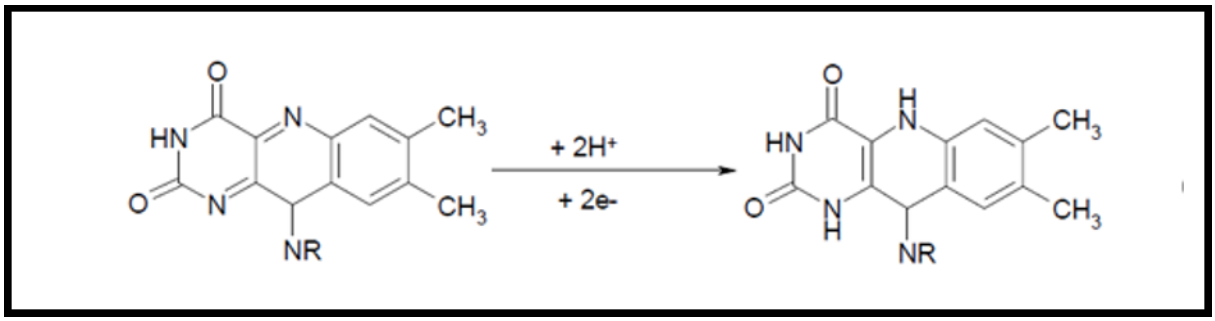

Fig 2.6. FAD being reduced to $FADH_2$.

The reoxidization process of $FADH_2$ back to FAD, sees "non-enzymatical" reaction of molecular oxygen producing hydrogen peroxide, as shown in fig 2.7.

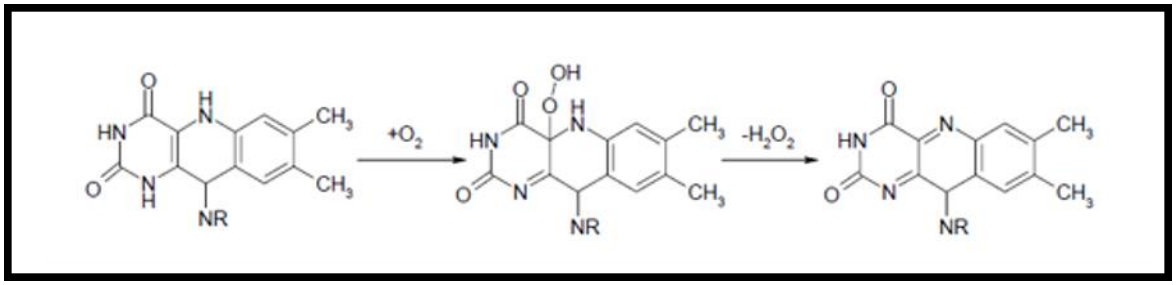

Fig 2.7. $FADH_2$ being oxidized to FAD.

FAD, in the presence of glucose, oxidizes glucose by carrying electrons from glucose to oxygen. The reaction for glucose oxidation catalysed by GOx is presented below:

$$FAD + (C_6H_{12}O_6) \rightarrow FADH_2 + (C_6H_{10}O_6) \quad 2.7)$$

$$FADH_2 + O_2 \rightarrow FAD + H_2O_2 \quad 2.8)$$

The oxidation reaction result of glucose by FAD produces $FADH_2$ and glucono-d-lactone. The $FADH_2$ is then regenerated by dissolved O_2 producing H_2O_2 and returning the enzyme to the FAD form.

2.4) Biosensors

Proposed in 1996 and accepted by IUPAC in 1999, a biosensor is defined as: "a self-contained integrated device that is capable of providing specific quantitative analytical information using a biological recognition element which is in direct spatial contact with a transducer element." [45] It is an analytical device converting biological responses into an electrical signals. The word 'biosensor' in a broad sense is used to cover sensors in which biological system might not be used directly but which do detect the concentration of compounds and other parameters of biological systems. Since then efforts have been made to fabricate biosensors for various infectious and non-infectious disease detection. [46, 47]

2.4.1) Characteristics of biosensor

Characteristics of biosensor	
Sensitivity	The change in biosensor response per unit change in concentration of target analyte
Selectivity	The ability to differentiate between the target analyte and other molecules in the sample
Linearity	The range within which the biosensor shows linear correlation to the target concentration
Response time	The time taken to respond to the target analyte
Shelf life	The time period in which the biosensor response does not deteriorate
Reusability	The number of times a biosensor can be used without any change in its response to the same analyte concentration
Accuracy	The ability to give the same response to the same target concentration when used repeatedly

Fig. 2.8: Characteristics of a biosensor.

2.4.2) Components of Biosensor

A biosensor typically consists of three major components: (i) bioreceptor or biorecognition element, (ii) immobilization matrix and (iii) transducer unit. fig. 2.9 shows the schematic of a biosensor.

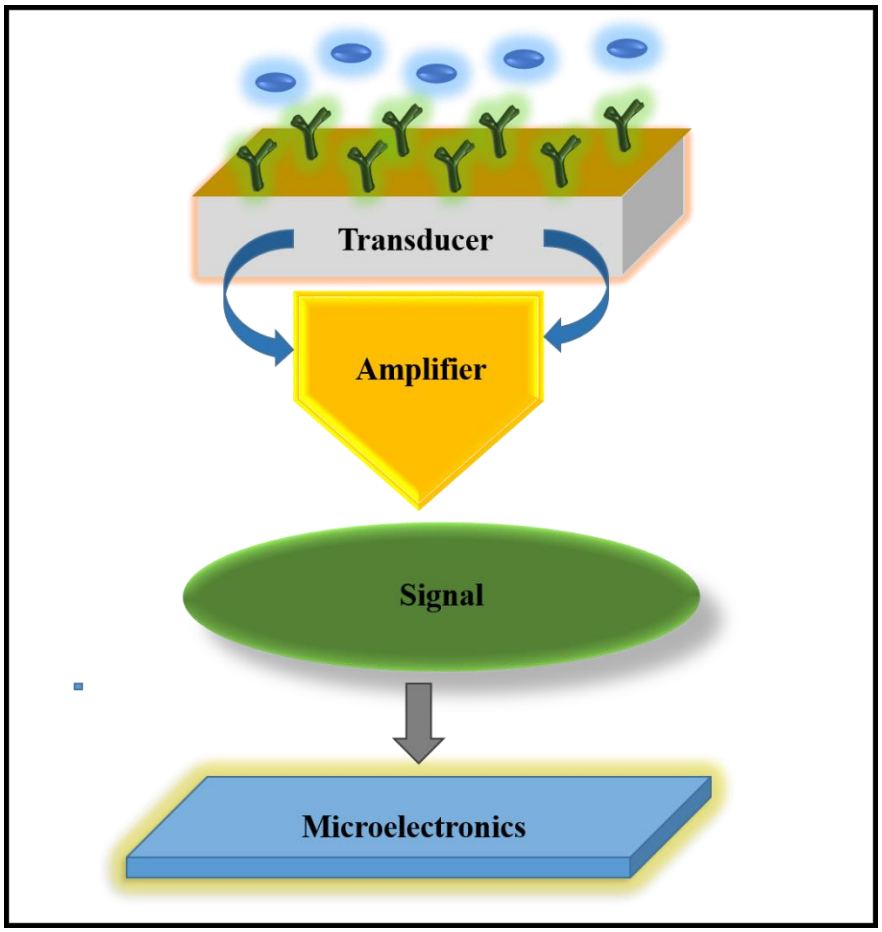

Fig. 2.9: Schematic representation of the components of a biosensor.

i) Biological recognition elements

The biological recognition elements or bioreceptors can be broadly categorized into two groups i.e. catalytic and non-catalytic. The catalytic group comprises enzymes, plant or mammalian tissue and micro-organisms while the non-catalytic class includes antibodies, nucleic acids and receptors. The transducer detects the resultant yield of the interaction.

ii) Immobilization Matrix

An Immobilization matrix supports the desired biomolecules by immobilization at the transducer surface while also maintaining stabilized environment for biomolecules and helps them retain their biological functions for a longer period. The choice of immobilization method to be used depends on the chemical properties of desired solid support which may include ionic strength, chemical composition, physiological pH, etc. Several techniques such as physical adsorption, covalent linkage, membrane entrapment, etc. can be used to immobilize the biomolecules onto the matrices. The physical methods of immobilization have major disadvantages such as long incubation time and non- reproducible results due to possible leaching of bio-molecules during washing. The covalent method of immobilization is more reliable due to the high stability of covalently bound biomolecules onto the solid surface leading to reduced non-specific binding. Several types of matrices including self-assembled monolayers (SAM), nanomaterials, sol-gels, and conducting polymers can be utilized for the immobilization process.

iii) Transducers

The physical part generating signals in a sensor is the transducer. These signals are the results of interactions between the sensing element i.e. antibody, enzymes etc and the target analyte, generated when analytes are recognized by the biological element. This biological interaction is then converted by transducer into a measurable signals. Depending on the type of transducer, biosensors can be grouped into three broad categories namely: electrochemical biosensor [48] (Ghindilis et al. 1998), the piezoelectric biosensor [49] (Chu et al. 1995), and optical biosensor [50] (Gauglitz 1996).

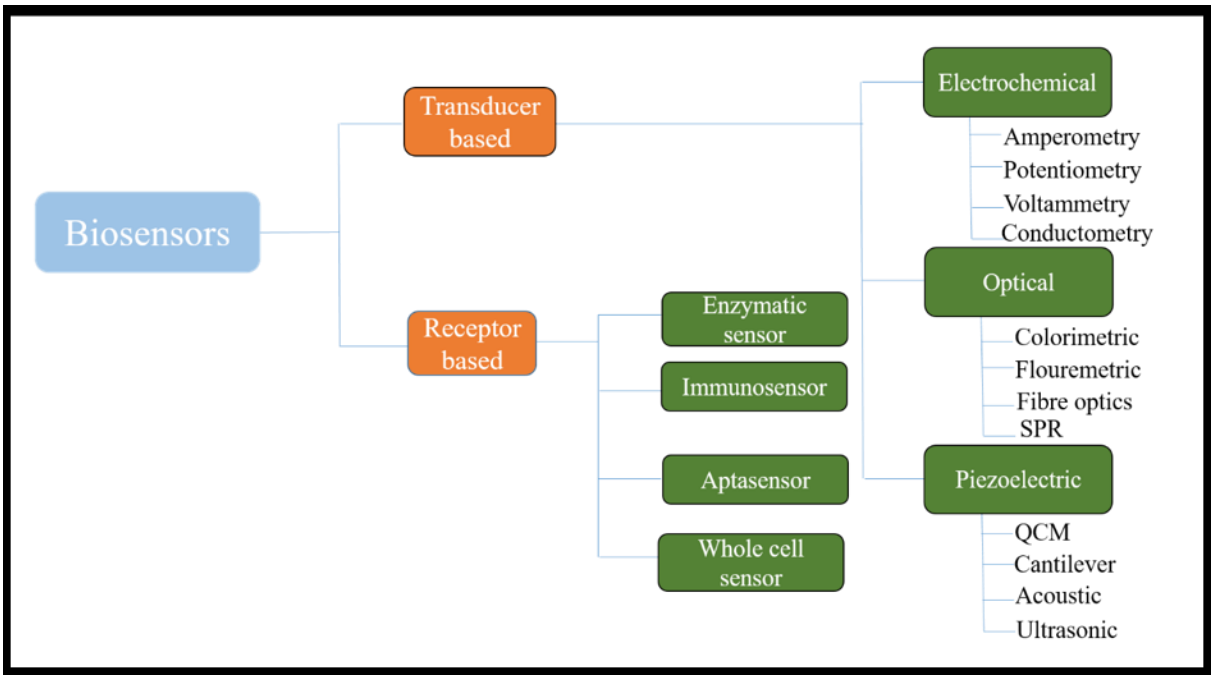

Fig. 2.10: Different types of biosensor.

2.4.3) Electrochemical biosensor

2.4.3.1) Electrochemical principles

Electrochemistry is the area of science which deals with the study of charge transfer process at interfaces and helps take electrical measurements of chemical reactions. The electron transfer process is represented as follows:

$$O + ne^{-} \leftrightarrow R \qquad 2.9)$$

where O = oxidized species, n = number of electrons transferred, R = reduced species,.

2.4.3.2) Capacitive current

The electrode possesses certain charge density due to an deficiency or excess of electrons at the surface of electrode. The electrical neutrality at the interface is maintained by both the electrolyte and solvent ions/dipoles need to be redistributed in such a manner that the charge in the solution nearer to the surface of electrode is equal but opposite, and these charge layers at the interface is known as an electrical double layer. Capacitive current (Ic) is generated across the

interface creating a capacitor associated with potential difference during the double layer charge separation.

$$I_c = C_{dl} \frac{dE}{dt} \quad 2.10)$$

I_c = total current measured in the experiment C_{dl} = double layer capacitance.

2.4.3.3) <u>Nernst equation</u>

The Nernst equation is basically used in electrochemical reaction to describe how the potential of the electrode depends on the activity of reduced (a_R) and oxidized (a_o) species

$$E = E^0 + \frac{RT}{nF} \ln \frac{a_0}{a_R} \quad 2.11)$$

Where E_0 = standard electrode potential of the electrochemical reaction which is defined as the electrode potential of reaction (eq. 2.9) when $a_o = a_R = 1.7$, T = thermodynamic temperature, R = the gas constant (8.3144621(75) J mol-1 K^{-1}), F = Faraday constant.

In electroanalytical experiments, concentration of the electroactive species is usually more significant than their activities. The given equation shows the relation between activity coefficient γ and concentration:

$$a = \gamma C \quad 2.12)$$

Thus, the Nernst equation for concentrations changes to:

$$E = E^0 + \frac{RT}{nF} \ln \frac{C_0}{C_R} \quad 2.13)$$

Where E^0 = formal potential.

$$E = E^0 + \frac{RT}{nF} \ln \frac{\Upsilon_0}{\Upsilon_R} \quad 2.14)$$

There are three main categories in which electrochemical biosensors can be classified based on the measurement of elelctrochemical properties.

i) Potentiometric devices measure the charge/potential collected at a given sensor surface with respect to a reference when no current flows and provides information on an ion activity.

ii) Conductometric/Impedimetric devices measure conductance/impedance change; generally, change of resistance or capacitance, at the sensor surface.

iii) Amperometric devices which measure current generated at the sensor surface from the electrochemical reduction or oxidation of an electroactive species, usually in response to an applied potential.

The device developed in this work is based on the amperometric biosensor. Since the reactions are detectable only in close proximity at the interface of the electrode. Thus performance of the electrochemical biosensor majorly depends on electrode. In amperometry when change of current is monitored, a external constant potential is applied externally, with the precise control over that potential. These amperometric sensors are based on a three-electrode system i.e. a working electrode (WE), a reference electrode (RE) and a counter electrode (CE). The WE works as the sensing electrode where the electrochemical reaction of interest occurs on the surface Commonly used WE are made of an inert material such as Au, Ag, glassy carbon, etc. The RE is commonly made up of Ag/AgCl and is placed at certain distance from the redox reaction site which maintain a known and stable potential. The potential of the electrode depends on the activity of chloride ions which is held constant by a saturated KCl or NaCl solution. While the CE is used for completing the circuit and it does not take any direct part in the redox reaction while establishing a connection to the electrolyte i.e. mediator so that a current can be applied to the WE. It can be made up of the same material as of WE. All of these three electrodes needs to be conductive as well as chemically stable.

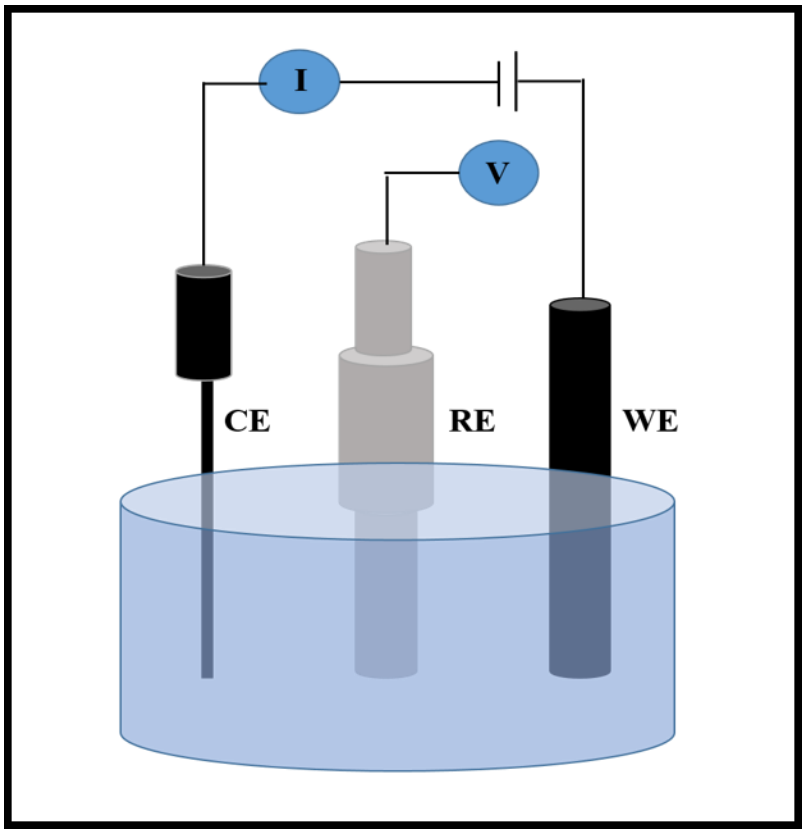

Fig. 2.11: Conventional 3 electrode system.

2.4.4) Piezoelectric biosensors

In these type of biosensors, there is a change in resonance frequency during biomolecular interactions and this change in resonance frequency is converted into an electrical signal which is proportional to the concentration of analyte present. This is exactly what this class of biosensor does. The piezoelectric biosensor not only offers ease of use, real-time output but also provide a wide pH range for working. [51] (Chu et al. 1995).

2.4.5) Optical biosensor

Optical biosensors are based on optical principles to convert a biomolecular interaction into a measurable analytical signal. The biomolecular interaction on the electrode surface changes the light characteristics of the transducer (i.e., intensity, phase, polarisation, etc.) and the biosensing process can measure the change in optical properties such as luminescence,

fluorescence, absorption or refractive index. These optical biosensors have several advantages such as multiple analyte detections at a time with a different wavelength, in vivo application.

2.5) Screen printing technology

The utilisation of solid metallic electrodes was a necessity within early days in the electrochemical experiments. However, over the time focus shifted towards the use of carbon-based materials within electrochemistry for the fabrication of low cost and miniaturized devices. This can be achieved with the exploitation of cheap and economical approaches such as carbon paste electrodes, which reduce cost significantly but can lack reproducibility. [52]

Since the early 1990s various printing approaches e.g. pad-printing, roll-to-roll and screen-printing have been utilized within the electrochemistry for the fabrication of electrode circuits.

Amongst all the above approaches, screen-printing technology has revolutionised the field due to their capacity to bridge the gap between laboratory experiments with in-field implementation. The screen-printed electrodes (SPE) has the capability for the mass production of the highly reproducible electrode configuration. [53].

SPE miniaturization can be done by fabricating all the three electrodes subsequentially on plastic, ceramic or silicone substrate. Such miniaturized electrode designs offer several advantages such as reduced sample volume, sensitivity, high current density (Ampere per area), the dominance of radial diffusion, low ohmic drop and signal-to-noise ratios, which has the potential for the replacements of conventional (solid and re-usable) electrode substrates. [54] [2 introduction].

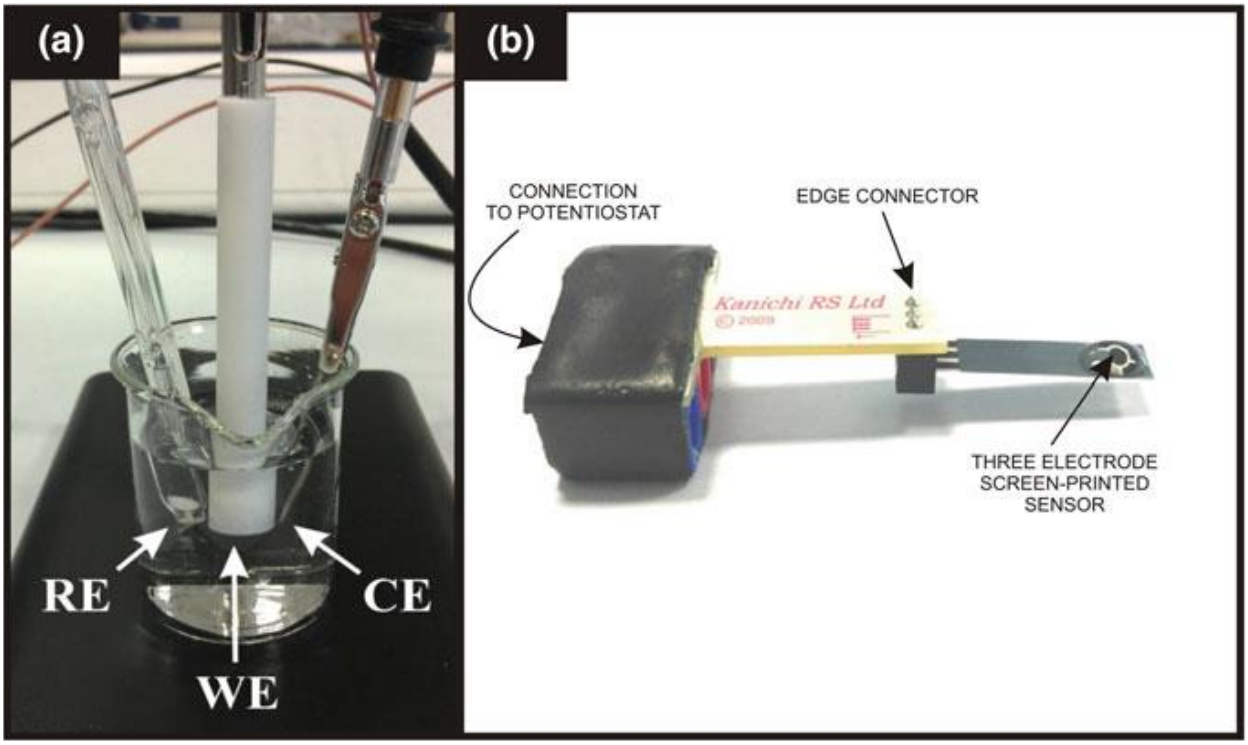

Fig. 2.12: depicts a traditionally used laboratory-based three electrode system compared to a system which has been printed using conductive inks; such a comparison indicates the ability to create electrochemical setups that are portable, cheap and reproducible.

Likewise, the commercially available electrochemical glucose biosensor, these screen-printed electrodes have been routinely used for other bio-sensing applications such as the determination of codeine within urine samples and diazepam in beverages. [55] [56], lactate sensing and cholesterol to name a few [57] [58]. Moreover DNA sensing using screen-printed electrode systems has turned into a large focus over the recent decade with much research centering upon the quantification of mutagenic DNA bases. [59] [60] [61] Seeing that the developed sensors are low cost, mass produced, and disposable this allows for the rapid non-intrusive detection of radiation damaged DNA [62]

One of the fascinating application of SPE include the determination of cancer biomarkers, with target upon an array of proteins released pre-tumour within the body. [63]

The great versatility presented by the screen printed electrodes lies in the wide range of ways in which the electrodes may be modified. The composition of the printing inks may be altered by the addition of very different substances such as metals, enzymes, polymers, complexing agents, etc. There is also the possibility of post-modifying the manufactured electrodes by means of depositing various substances on the surface of the electrodes such as metal films, polymers, or enzymes [64].

In current applications, graphite materials are preferred for electrodes due to their simple technological processing and low-cost, although other materials such as gold and silver-based inks are also used for analysis and determination of various elements

2.5.1) Screen-printed designs

From manoeuvring of the working electrode material through the use of screen printing techniques, the electrode geometry is instantly customised through the incorporation of screen-printing technologies for the development of electrochemical sensing platforms. When we design such platforms, it is appropriate to have electrodes which do not require a large sample size. The geometry was designed as close as possible to minimize the resistance between working electrode (WE) and a reference electrode (RE). The area of counter electrode was designed to be larger than the area of working and reference electrodes which allow unlimited current transfer in the circuit. All the channels of the electrode geometry were designed with a graphic software (Corel Draw X8). Our electrode configuration is the 5 mm working electrode dia with on-chip reference and the counter electrode. The dimension of the connecting pads at the end of the electrode is 5 × 1.8 mm. For reproducibility, ensure the electrode position is aligning onto the channel.

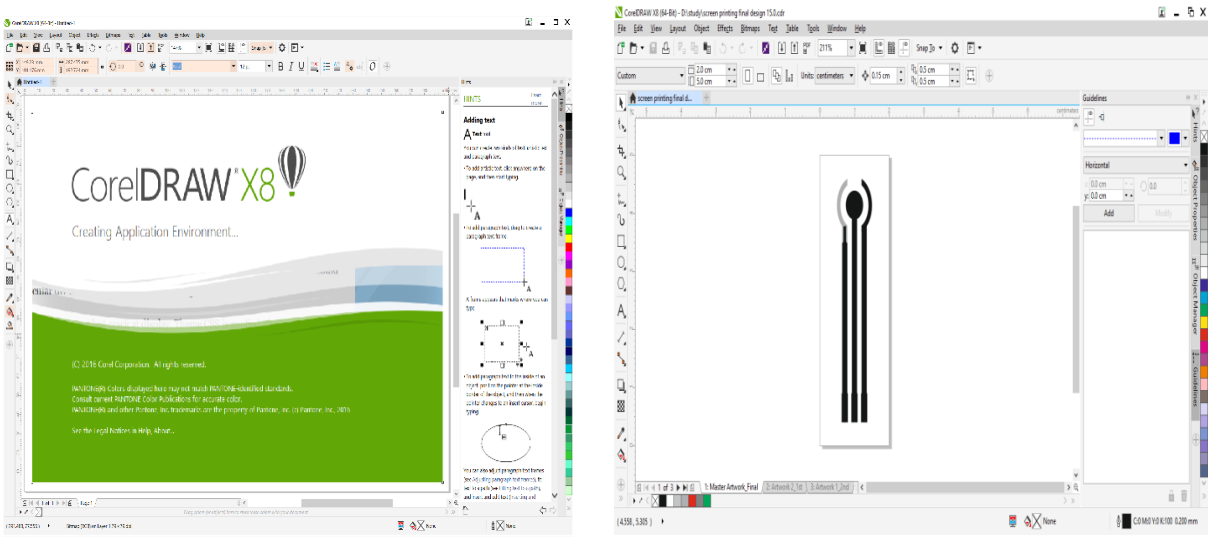

Fig. 2.13: Designing of Screen Printed Electrodes in Corel Draw.

2.5.2) Printing media

The usage of a printing medium (i.e. ink or paste) within the screen-printing procedure is vital for the transfer of the printed design, mostly these inks or pastes are readily manufactured using conductive particles within a solvent/binder mixture to permit the transfer of the particulate matter onto the PET substrate. These inks are beneficial to the user as they possess the ability to tailor or manipulate the working electrode compositions.

Wang et al. [65] showed that the choice of carbon ink should depend upon the application at hand, due to the differences in the electrochemical signals seen with a range of inks [66]. Such other examples of printable inks, include the fabrication of platinum [67] and gold [68] screen-printed sensors which have been applied towards the electroanalytical sensing of chromium species (VI and II) in the case of the gold sensor, and both hydrazine and hydrogen peroxide for the case of the platinum sensor [69, 70]. Crucially, it was determined that the requirement for electrode potential cycling prior to utilisation (as is the case for bulk noble metal macro electrodes in order to form an oxide upon the electrode surface) was alleviated in the case of the screen-printed sensors owing to the noble metal utilised within the screen printing process being in the

form of an oxide [71, 72]. Clearly, the removal of such a preparatory step offers significant benefits when considering the development of sensors intended for use outside of the laboratory environment where rapid and facile analysis is imperative (one-step analysis). However, mentioned previously the metallic options can be costly and the need for carbon-based materials has become necessary. In response to this, the utilisation of graphitic based inks for an assortment of applications has been realised. Not only do these inks replicate the electrochemistry of typically used electrodes such as glassy carbon (GC) and edge plane pyrolytic graphite (EPPG) but they are manufactured at a fraction of the cost. Also, an array of carbon materials can be used, such as carbon nanotubes [73], graphene [74], mediated carbon structures [75] and nanoparticles [76] to name a few.

Having the ability to alter the electron transfer capabilities at an electrode surface has a beneficial effect on the analytical applications. Shown in Fig. 1.8 compares the voltammetric behaviour of unmodified screen-printed electrodes with that of the polymeric modified screen-printed electrode; upon the metallic plating of these systems, the electrochemistry will be dominated by the metallic properties rather than the underlying electrode.

2.5.3) Substrate

One aspect of screen-printing technology, particularly in the case of the fabrication of electrochemical devices which is often overlooked, is the selection of the electrode substrate on which the ink is printed upon. Screen-printed electrodes are generally printed upon ceramic [77, 78], or plastic substrates [79, 80] and the need for ultra-flexible sensors has arisen due to the possibility of using the screen-printed electrodes not only just within the laboratory environment but within the scientific field outside its confines applied “into-the-field”.

Wang et al. [81] developed wearable electrochemical sensors on underwater garments comprised of the synthetic rubber neoprene. The neoprene-based sensor was evaluated towards the voltammetric detection of trace heavy metal contaminants and nitro-aromatic explosives in seawater samples.

Fig. 2.14: Optical images of the electrochemical tattoo upon the substrate and skin.

2.5.4) Screen printing process

The technique of screen-printing is described as the production of thick film hybrids, for applications within many areas of the scientific community, such as circuit boards and electrochemical systems to name a few. Due to the nature of screen-printing the creation of mass-produced thick films can be realised, with the utilisation of relatively cheap and simple designs, this process possesses excellent scales of economy. Additionally, it can be noted that due to the simplicity of the machinery used throughout, this process can be altered and changed upon a fundamental understanding of screen-printing.

The process of screen-printing typically consists of five prerequisites to ensure identically reproducible thick films; these are as follows:

i. Suitable printing medium
ii. Mesh screen with an embedded stencil design
iii. Substrate to print upon

iv. Flexible and resilient squeegee

v. Secure base to prevent movement of the substrate within the process.

It is important to note that suitable printing machinery is desired to ensure the desired level of reproducibility is achieved with a high throughput. Nevertheless, there are situations where the printing machinery can impede and become inauspicious to the overall screen-print, it is with these considerations that it is solely reliant on the methodology.

2.6) Paper

Papyrus, the word originated in Latin which means the paper, is one of the most valuable invention for humankind. Cellulose is the main constituent of the paper, and the chemical formula of this organic compound is $(C_6H_{10}O_5)_n$. It is a natural polymer composed of a linear chain of β(1→4) linked D-glucose units and joined by β(1→4) glycosidic bond. Paper can be manufactured by extracting water from pulp, and the filtration is followed by pressing and heating. The pulp is chiefly produced by isolating the wood into its constituent fibres in a chemical, mechanical or thermochemical thermomechanical, or chemical process [82]. Fig. 2.15 shows the structure of the cellulose fibres**.**

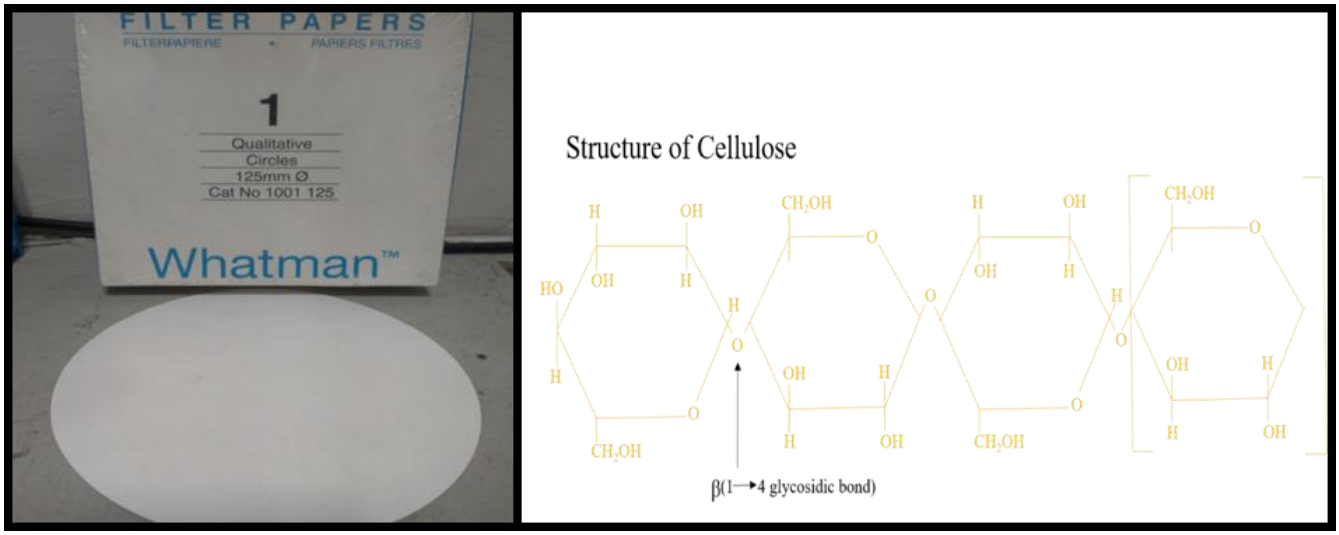

Fig 2.15: Whatman filter paper and the structure of cellulose

Paper is a flexible, lightweight, low-cost, recyclable and biodegradable material while first it is utilized for the packaging, displaying and storing information. However, in due course of time researchers have discovered more extensive applications in filtration (Whatman paper), as an actuator, and also used as a transformer (as a dielectric material).

In recent years filter paper has been utilized as the substrate material for low-cost, flexible electronics such as supercapacitors, batteries, and in biosensing applications [83]. Paper has opted as a substrate material because it has a large roughness, poor mechanical and chemical barrier that allows it to absorb conducting materials into its porous structure. Also, it can be chemically modified chemically to incorporate various functional groups that can vary the bulk and surface properties of paper [84, 85].

Herein, we describe the cellulose paper as an electrochemical cell. In recent applications paper was reported as the reagents storage matrix used in electrochemical detection. The combination of paper for prestorage of reagents with electrochemical detection creates one-step detection of the analyte. [86]

The immobilization techniques play a vital role in stabilizing the enzyme because the enzymes generally don't have the long-term stability which also determines the overall performance of the biosensors. These enzymes can be reused after attaining the stability. For the development of biosensor, there are various techniques such as entrapment, physical adsorption, encapsulation and entrapment, ionic, covalent and cross-linking for enzyme immobilization. These techniques require large quantities of enzyme and also there is a loss of enzyme activity from the electrode surface resulting in a short lifespan. Thus there is a need of simple and efficient immobilization of glucose oxidase for the fabrication of glucose biosensors for on-site process monitoring. Fine fibre matrix containing cellulose paper is ideal for immobilising enzymes, and

its highly porous microstructure provides a suitable matrix for enzyme immobilization through simple adsorption technique.

The whatman filter paper was used due to its various properties, such as wettability and good porosity; supported by ion exchange properties of the whatman paper. Whatman paper quickly adsorb the sample solution which dissolves the prestoraged reagents and thereby covers the surface of the electrode. Due to the excellent wettability properties of paper it makes good contact with SPE. The paper does not require any adhesive to make contact with SPE because of surface tension properties of water on paper.

2.7) Nanomaterials

Nanotechnology, defined by the royal society is the "Design, characterisation, production and application of structures, devices and systems by controlling shape and size at the nanometer scale". In nanoscale, the properties of the materials are different from the material of larger scale. Nano means "dwarf" in Greek. [87]

Two principal methods for synthesising nanoscale materials i.e. the top-down & bottom-up have entirely distinct fabrication technique. The top-down nanofabrication begins with a big structure and makes it smaller through successive decrease in size while the bottom-up nanofabrication begins with single particles and makes them up to a nanostructure. However, at nanoscale the properties of constituent material changes. Some materials used for electrical insulations can become conductive, and other materials can become transparent or soluble. We can also observe that gold nanoparticles have a different colour, melting point and chemical properties, due to the nature of the interactions among the atoms that make up the gold, as compared to the bulk of gold. Also nanosize gold is physically different from the bulk gold, and depending on the size of the particle it can be orange, purple, red or greenish (Ratner & Ratner, 2003) [87].

Two of the major factors which are responsible for why nanoparticles have different properties, i.e. optical, electrical, magnetic, chemical and mechanical than the bulk material, are size-range quantum effects which start to predominate and the surface area to volume ratio which get increased (Holister et al., 2003) [89]. The increase in the surface-area-to-volume ratio is a gradual progression as the particles get smaller which leads to those atoms on the outside of the particle will increasingly begin to dominate the ones inside the particle. This changes the individual properties of the particle and how it interacts with other materials in the surroundings. The large surface area enhances the mixing of other materials in the surrounding which is beneficial in intermixed materials like composites.

The commercial application of nanotechnology has been accomplished for bulk products, such as cosmetics containing nanoparticles having the capability to target deeper into the body, and sunscreens with increased transparency, etc. The cosmetic company like L'Oreal has done impressive work on nanotechnology while improving their existing products which are exclusively patent by them(Wood et al., 2003) [90]. Also, nanoparticles as fillers have been introduced in the composite materials with an enormous market such that nanoparticles can change the properties of the material as it hardens the metal and softens the ceramics. Automotive and aerospace industries have developing potentials of nanoparticles where they already been introduced in the "GM Motors Safari and Chevrolet Astro ." (Wood et al., 2003) [90].

Medical applications always remain the field with the biggest expectations regarding human welfare. With the development of new materials and introducing their application in biotechnology, it could be possible to make artificial organs and implants through cell growth which could further repair damaged nerve cells, replace damaged skin, tissue or bone (Wood et al., 2003) [90].

Nanomaterials of carbon especially graphitic nanomaterial have sparked enormous interest in the recent years because of the discovery of several new materials with unique properties. [91-93]

Graphene Oxide (GO) is a wrinkled two-dimensional carbon material consisting oxygen functional groups on its basal plane and edges. [94] These oxygen functional groups confers a hydrophilic character of GO while graphene is a hydrophobic material. Electronic, mechanical, and chemical properties of GO is strongly affected by oxygen functional groups, therefore, resulting in the property differences between GO and pristine graphene [95]. rGO showed superior electrochemical behaviour such as large voltammetric current and lower oxidation potential that makes it a perfect material for electrochemical biosensing.[96] It has been widely explored for the development of electrochemical biosensors whose conductivity is usually enhanced by several orders of magnitude during the reduction processes. Excellent in electrical conductivity also with improved thermal conductivity, high surface area (theoretically 2630 m^2/g for single-layer graphene) and strong mechanical strength [97] place the rGO for use in many applications, including electronics [98], solar cells [99],fuel cells [100, 101] as well as energy storage and conversion devices, such as supercapacitors [102, 103] and batteries[104-107]. Apart from brittle graphite, rGO sheets are flexible, which is an advantage for fabrication of flexible electronic and energy storage devices.

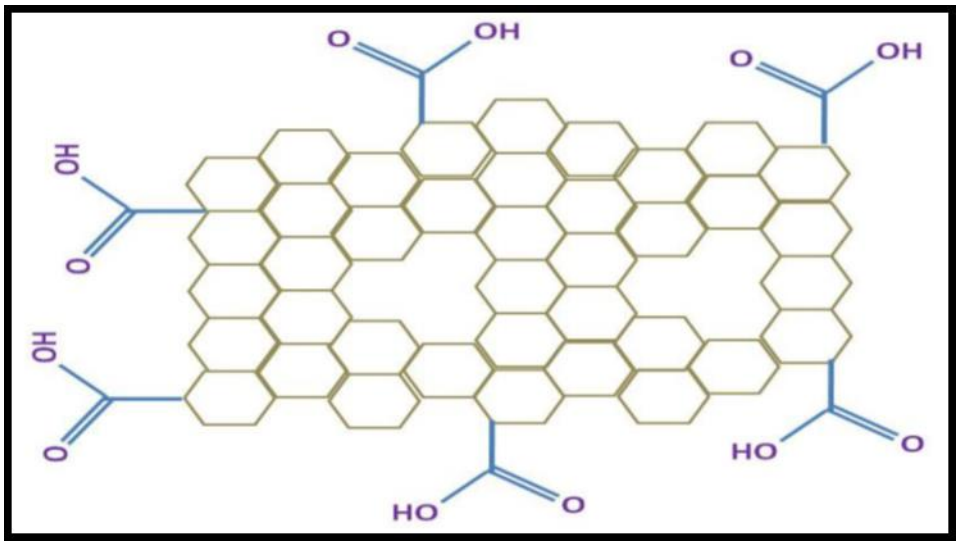

Fig. 2.16: Structure of reduced graphene oxide.

3) Materials & Methods

3.1) Apparatus

Semi-automatic screen printing machine from APL Machinery Pvt Ltd, Faridabad. The cyclic voltammetric experiments were carried out with an Electrochemical analyser (AUT-85279, Metrohm, India). The screen patterns were designed with Corel draw software X8, and mesh screens were generated by D. R. Optical Disc Pvt Ltd, Mayapuri, New Delhi. These experiments were conducted on SPE of graphite paste as working & counter electrode, Ag/AgCl paste as a reference electrode in phosphate buffer saline (PBS, 0.1 M, pH 7.0) containing 5 mM $[Fe(CN)6]^{3-/4-}$ with 0.9% NaCl. Scanning electron microscopy (SEM) was performed by using S-3700N. X-ray diffraction (XRD) have been carried out in a X-ray diffractometer (Bruker N8 Advance). UV-vis-NIR absorption spectra of graphene oxide solution was measured with Perkin Elmer Lambda 950 UV-vis-NIR spectrophotometer. Ultrasonicator from PCI Analytics Pvt Ltd with Operating frequency of 33 ±3 KHz has been used for sonication at room temperature.

3.2) Reagents and materials

Graphite, silver and Ag/AgCl paste was purchased from BHEL, India. Graphite powder, D-glucose and the stock solution of glucose oxidase, from Aspergillus niger were purchased from Sigma-Aldrich. Filter paper no. 1 was procured from Whatman. 0.1 M phosphate buffer solution (PBS) was prepared from 0.2 M Na_2PO_4, and NaH_2PO_4 in autoclaved DI water and adjust the pH to 7. All the experiments were conducted at room temperature (25 $\pm 2^0$C).

3.3) Designing of SPE

From manoeuvring of the working electrode material to the electrode geometry, the incorporation of screen printing technique is beneficial for the development of electrochemical biosensor. The electrochemical biosensing platform is designed in such a way that small sample

size is required to carry out the experiment. The geometry was designed as close as possible to minimize the resistance between working electrode (WE) and a reference electrode (RE). The area of counter electrode was designed to be larger than the area of working and reference electrodes which allow unlimited current transfer in the circuit. All the channels of the electrode geometry were designed with a graphic software (Corel Draw X8). Our electrode configuration is 5 mm WE dia with on-chip RE and CE. The dimension of the connecting pads at the end of the electrode is 5 × 1.8 mm. For reproducibility, ensure the electrode position is aligning onto the channel.

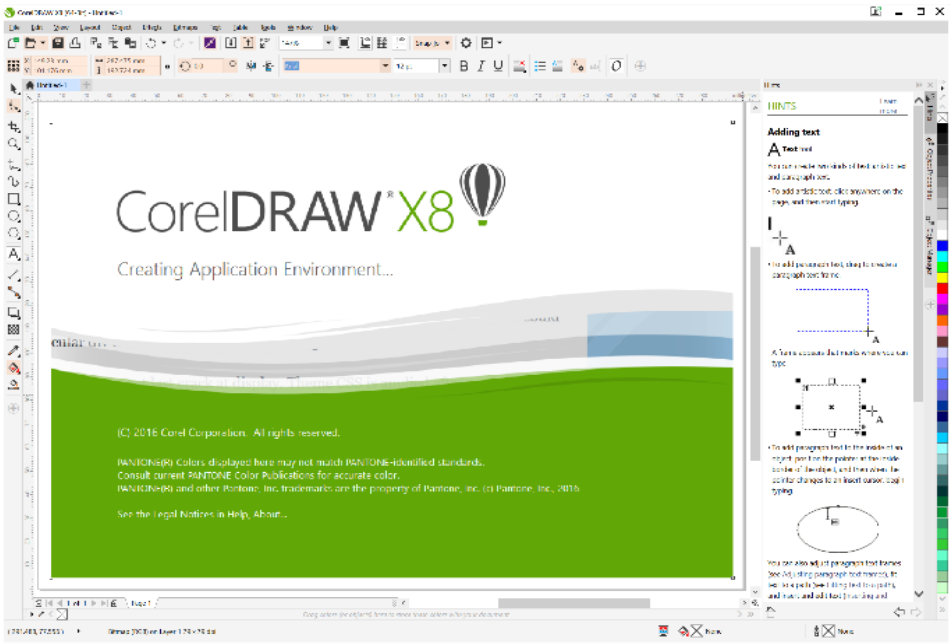

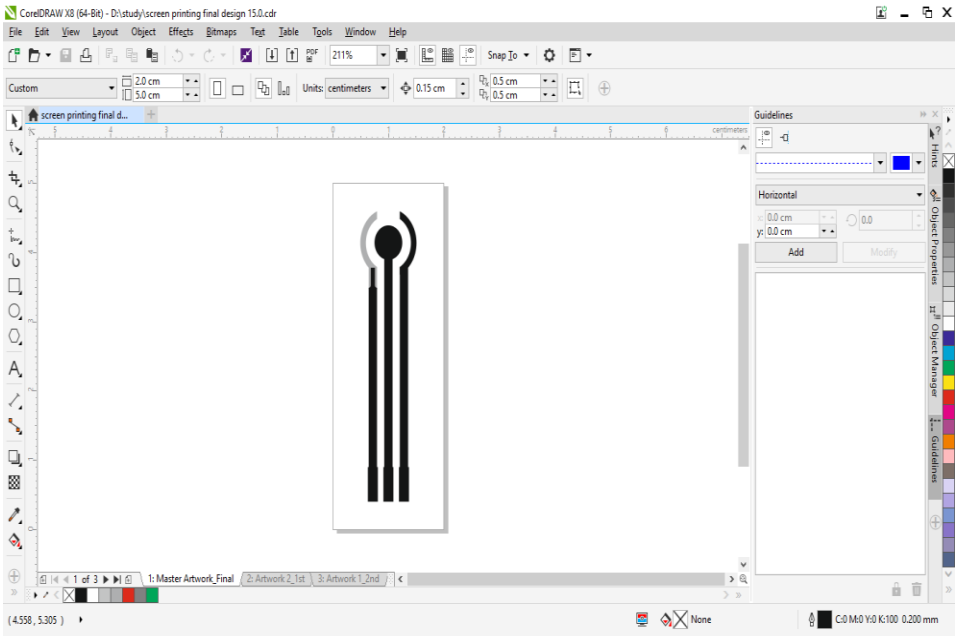

Fig. 3.1: Designing of Screen Printed Electrodes in Corel Draw

3.4) Fabrication of Screen-Printed Electrodes

The SPEs are fabricated with the help of screen- printing technology, which comprises of a layer-by-layer deposition of conducting or non-conducting paste upon a solid substrate. In screen printing, the paste is spread uniformly onto the substrate by using a squeegee through a mesh screen. The dimensions of SPE is defined ny the patterns (negative) on the mesh screen.

Basic stages of the fabrication of SPE:

(i) Selection of mesh screen defining the dimensional features of SPE

(ii) Preparation of paste

(iii) Substrate selection

(iv) Printing of SPE; and

(v) Curing of fabricated SPE

SPEs were fabricated with the silver paste, graphite paste and silver/silver chloride paste onto a PET substrate. All the three electrodes were situated throughout the channel allowing the contact with the solution so as to achieve the electrochemical detection.

i. In the initial step, we select the appropriate mesh screen in order to obtain layers of different ink onto the substrate.

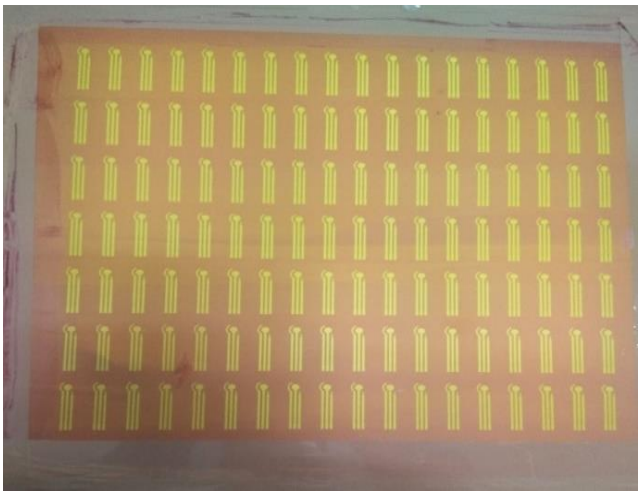

ii. The screen is picked up by holding the frame. Do not touch the meshso that the screen is not damaged or contaminated.

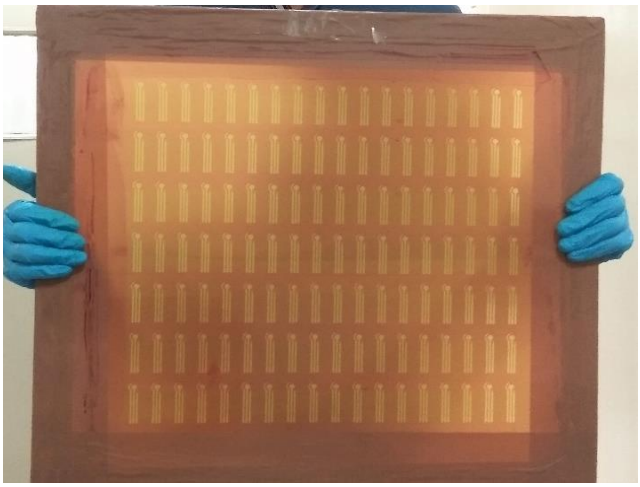

iii. Carefully place the screen into the semi-automatic screen printing machine and ensure that the top portion of the screen is facing down.

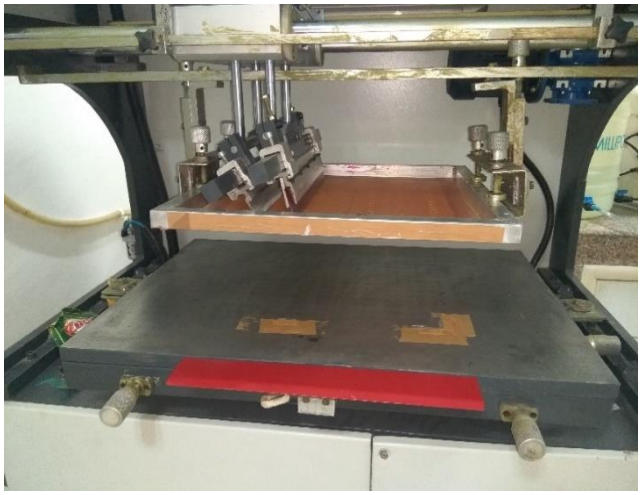

iv. After settling the mesh screen into the machine, the first layer of silver paste referred to as conducting path can now be prepared. The paste is viscous therefore it requires mixing to create a homogenous mixture. Mixing can be either done mechanically or by hand or mechanically.

v. When the paste is ready, apply it alongside the design of SPE on mesh screen with an adequate quantity to print the desired quantity of electrodes, subsequently reducing the wastage of paste as well as cost of SPE.

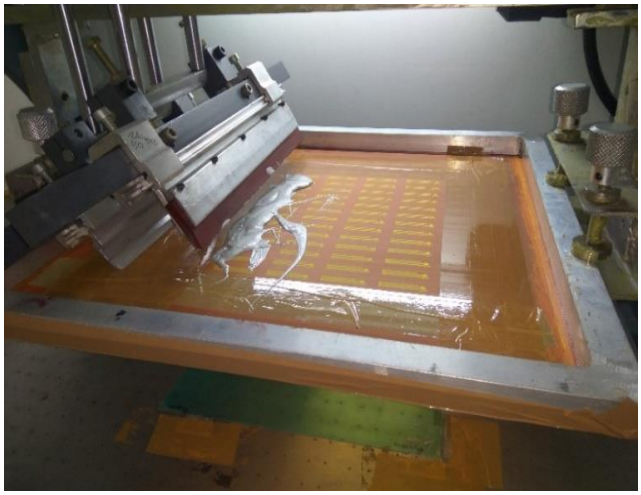

vi. Place the PET substrate on the surface of the bed considering that each layer overlays to provide a reproducible results.

vii. Printing cycle can begin by selecting menu and tap the multi-coating ‘ON’ button and after that START, upon this guideline, the machine will pull up the bed and start the cycle. At first, the paste is dragged by flood bar over the mesh screen, then the squeegee applyies a pressure by which the paste is forced to pass through the stencil design.

viii. After the first cycle, the conducting path design is transferred on top of the substrate. Look up for the areas that remains unprinted or uneven coverages.

ix. To complete the process, place the sheet in an oven for curing of the paste at 120^0C for 30 min.

x. Upon accomplishing the first layer, put the second screen for working and the counter electrode and load graphite paste onto the screen. repeat the above mentioned procedure to run the printing cycle for second layer. When the screen removed from the substrate, it leaves behind ink that dries to yield a working and counter electrode.

xi. Curing step for 30 min at 120^0C was needed.

xii. Now place the third screen in the similar fashion for the reference electrode and load Ag/AgCl paste onto the screen. Place the same command of multi-coating as mentioned in the previous two steps.

xiii. Place the sheet in the oven for 30 min at 120^0C for curing.

xiv. Approximately 30 electrodes were printed on each sheet at once and were cut into the individual electrodes.

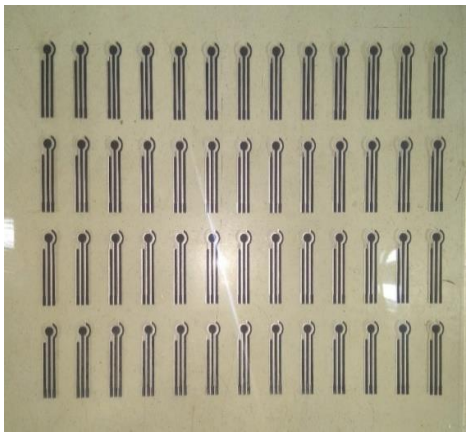

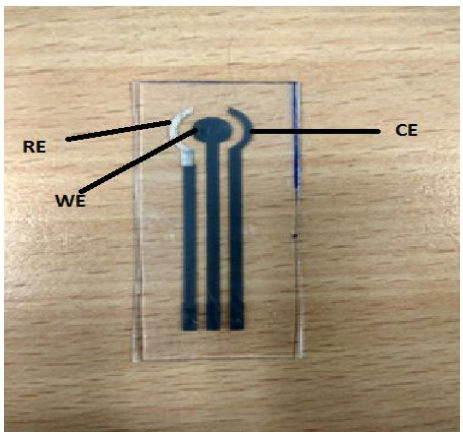

xv. To increase productivity, clean all the screens with Amyl (ink reducer) while the electrodes are curing. While cleaning the screen, apply mild force was applied on the underside and this did not affect the stencil design. However, serious care is taken while cleaning the top of the screen so as to not damage or contaminate the screen mesh.

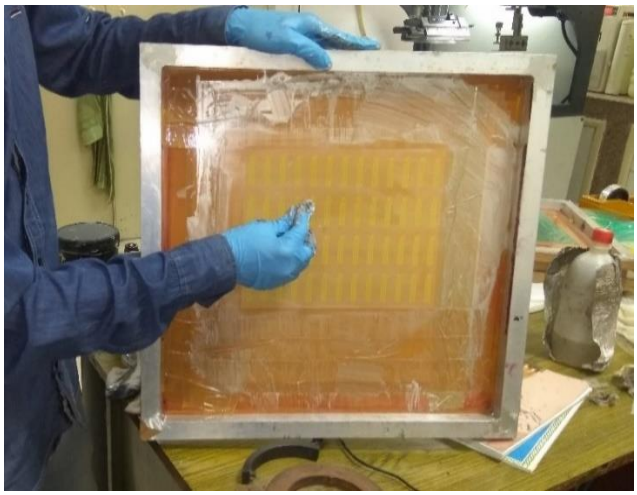

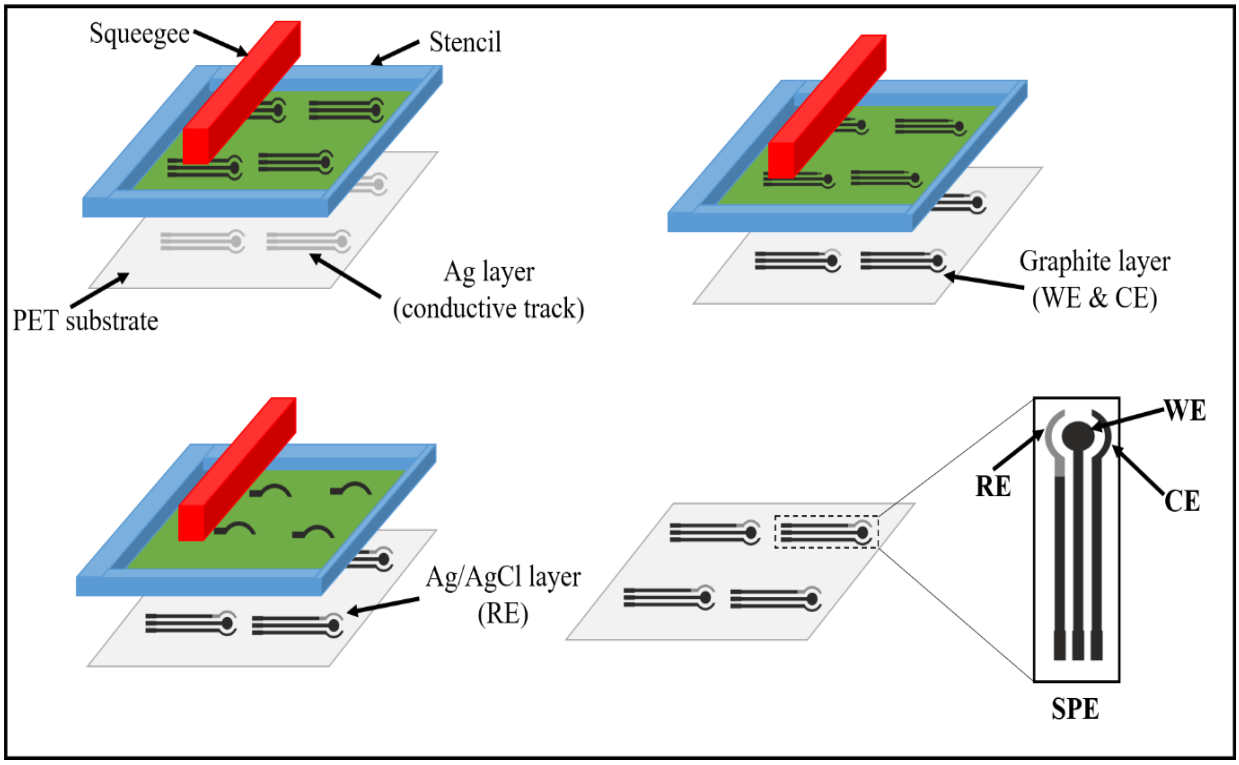

Fig. 3.2: Schematic representation of the fabrication of SPE.

3.5) <u>Pretreatment of SPE with NaOH</u>

For the proper adhesion of carbon paste onto the PET substrate, manufacturer add insulating polymers into the paste (composition of paste is unknown as producers did not reveal

it). These insulating polymers may result in an increase in the electron transfer resistance. By pretreating the SPE, our aim is to remove the insulating polymers and increase surface roughness. In the procedure, the fresh SPE were soaked into 3M NaOH solution for 1 hour as chemical treatment, washed with DI water and then cure the SPE at 120^0C for 15 minutes for 2-3 times.

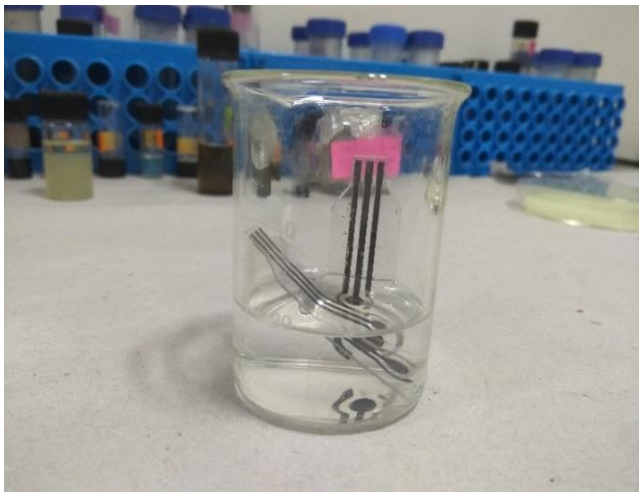

Fig. 3.3: Chemical treatment of SPE.

3.6) <u>Preparation of Graphene Oxide (GO)</u>

GO was synthesized from graphite flakes by the modified Hummer's method. This technique typically consists of the preliminary oxidation of graphite flakes into graphite oxide; which is followed by mechanical, chemical or thermal exfoliation of graphite oxide to GO sheets. This exfoliation of graphite oxide in the vigorous condition results in the synthesis of graphene oxide. Briefly, 1.5 g of graphite flakes were initially oxidized by reacting with a mixture of 40 ml of 98% H_2SO_4 (sulphuric acid), 5g of $K_2S_2O_8$ (potassium persulphate) and 5g of H_3PO_4 (phosphoric acid) for 4 h at 80^0C. Further the prepared suspension was washed 4-5 times with DI water and is vacuum dried at 50^0C. To further oxidize the pre-oxidized graphite flakes, the obtained powder was added into a mixture of concentrated H_2SO_4: H_3PO_4 (180:13) under constant stirring. After 5 min, add 9 g of KMnO4 (potassium manganate) to the mixture and proceed with the stirring

for 15 h at 50^0C. After 15 h the reactants were allowed to cool down to room temperature following which 200 mL of ice was poured into the mixture. Then 1.5 mL of H_2O_2 (30%) was added. After this treatment with H_2O_2 the resulting suspension turned bright yellow, as it reduced the residual permanganate and manganese dioxide to the colourless soluble manganese sulphate. For the reduction of residues the material was then separated by filtration. Then centrifuge the filtrate at 5000 rpm for approx 3 h, and washing is done several times by DI water, 30% HCl and ethanol (100 mL of each) and then followed by centrifugation separation. Final sedimented pellet is suspended into 100 mL of ether and is filtered through a PTFE membrane. Thus the obtained semi-solid material as graphene oxide (GO) was vacuum dried overnight.

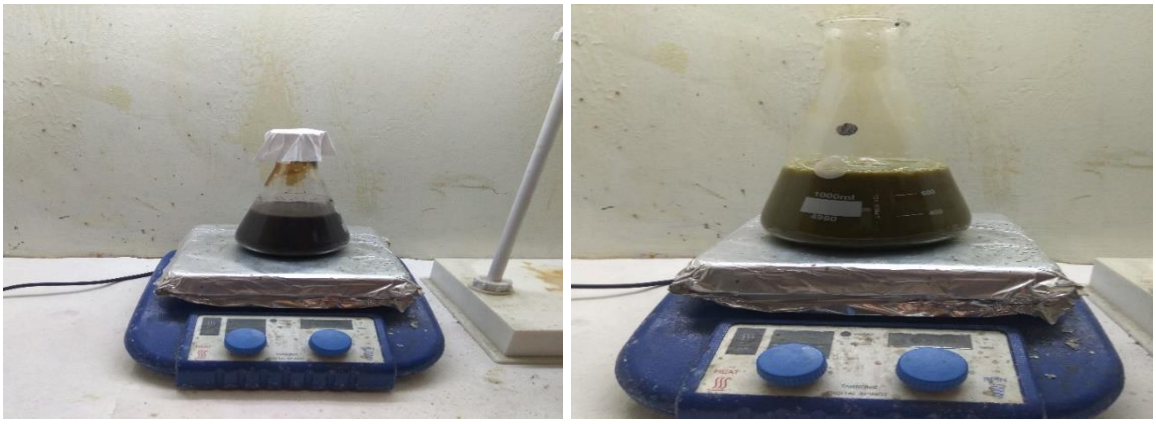

Fig. 3.4: Synthesis of Graphene Oxide.

3.7) <u>Modification of paper disc with GO-GOx composite</u>

We have functionalized GO with GOx and then reduce the GO electrochemically into rGO. GO-GOx biocomposite was prepared by dispersing 40 µl of GO (0.5 mg/ml in DI) into 60 µl of GOx (10 mg/ml in PBS, pH 7). The dispersion was sonicated for 30 minutes, to produce GO-GOx biocomposite. Then we add 30 µl each of EDC-NHS to the biocomposite for stability. Whatman filter paper no. 1 was used for the preparation of electrochemical cell (reagent storage device) and was cut into a round sheet with the diameter of 1 cm. 20 µl of the GO-GOx composite was drop

casted uniformly onto the paper disc . The uniform dispersion of GO-GOx occurs due to the capillary wicking and allowed to dry at 4^0C. Then to remove the loosely attached GO or GOx particles rinse the paper disc with DI water. By performing continuous potential cycles (15 cycles) from 0 to -15 V at a scan rate of 50 mV/s, GO in GO-GOx composite was electrochemically reduced to rGO.

3.9) Electrochemical determination of glucose with modified paper disc equipped SPE

The potentiostat used in this work is AUT-85279, Metrohm, India. Cyclic voltammetry is performed for characterization of modified paper disc equipped SPE using phosphate buffer saline (0.1 M, pH 7.0) containing 5 mM $[Fe(CN)_6]^{3-/4-}$ with 0.9% NaCl. The experiments were conducted at room temperature. 20 µl of glucose solution of different concentration (50-500 mg/dl) was added at different modified paper discs and left to air dry. Then paper disc was placed onto the surface of the SPE so as to cover all the three electrodes fully. For the determination of glucose, 50 µl of 1M PBS (pH 7) was dropped onto the centre of the paper disc and incubate it for 2 minutes to dissolve reagents and equilibrate the enzymatic reaction.

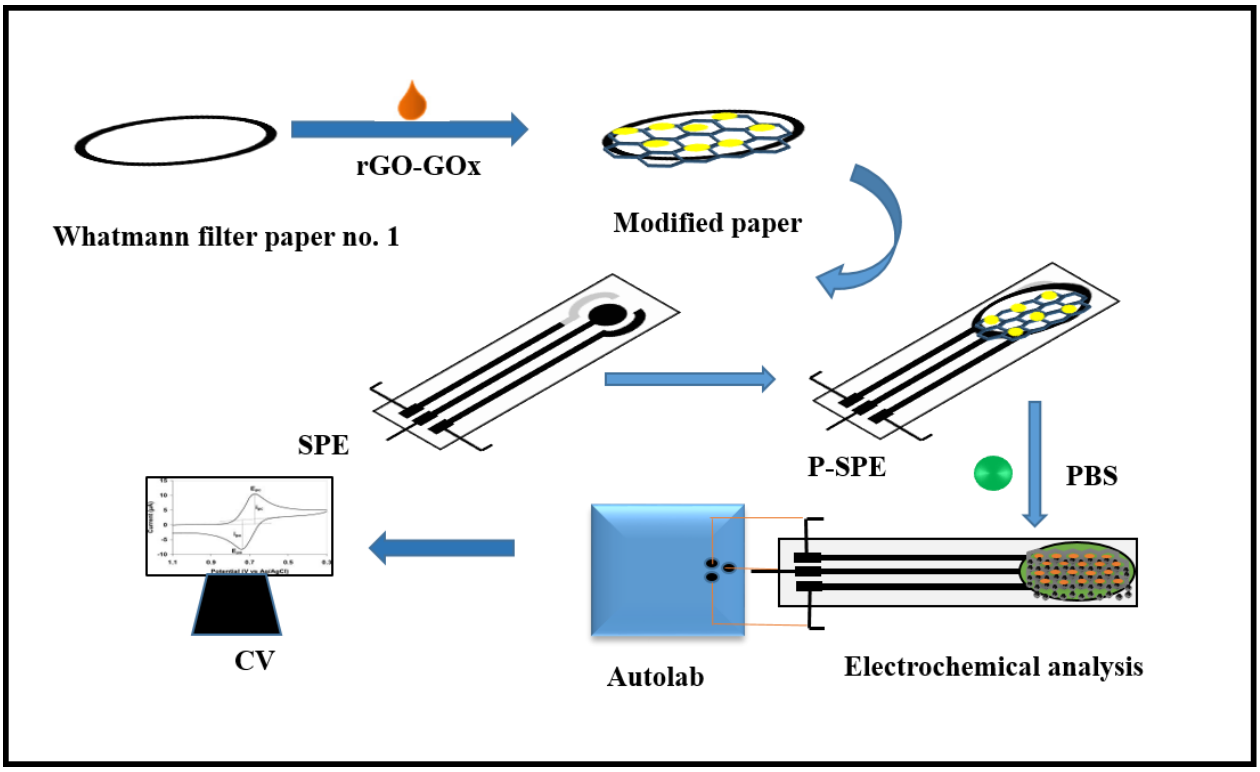

Fig. 3.5: Schematic of GO-GOx modified paper disc equipped SPE for Glucose Detection.

3.10) Instrumentation

3.10.1) Semi-automatic Screen printing machine

Semi-Automatic Screen Printing Machine with Stainless Steel Vacuum Bed with a print area of 20”x30” (55x80 cm) was used to perform the screen printing process. APL Machinery Pvt Ltd, Faridabad provided the screen printer having the finest, most flexible range of trouble free flatbed screen printing machine available. Although being a heavy duty machine, it is easy to set up and control giving maximum stability and accuracy at the full production speed necessary for high-quality screen printing. The Squeegee head on a solid steel shaft along with linear bearing motion provides accurate and vibration free squeegee movement.

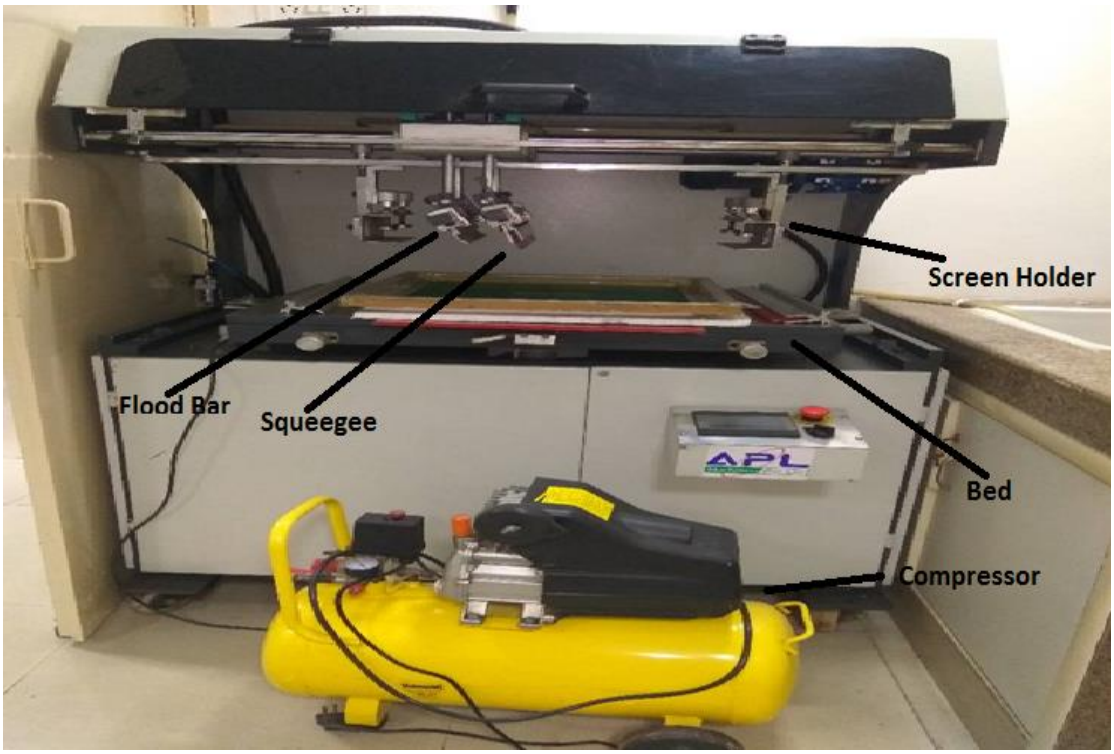

Fig. 3.6: Semi-Automatic Screen Printing Machine.

The substrate is printed on a flat table or a flat vacuum table where the squeegee is in motion, the screen and the substrate are stationary. This machine has unique aluminium frame profile to

overcome the problem of higher off contact. The mesh screen is placed on top of the frame holder which ranges from 3-5 mm thick giving it excellent stability. Some gap is kept between the substrate and the mesh screen since frame holder should not be in contact with the vacuum bed further increasing the off-contact distance.

3.10.2) <u>Electrochemical analyser</u>

All the electrochemical studies reported were conducted on an Autolab Potentiostat/Galvanostat (Metrohm, The Netherlands).These studies were carried out using a screen printed electrode with graphite as the working and counter electrode, and Ag/AgCl as a reference electrode. PBS solution (0.1 M; pH 7) containing 5×10^{-3} M $[Fe(CN)_6]^{3-/4-}$ as redox species was used as an electrolyte.

Fig. 3.7: Autolab Galvanostat/Potentiostat (Metrohm, The Netherlands).

Electrochemical techniques relate the changes of an electrical signal at an electrode surface by an electrochemical reaction, usually as a result of an imposed potential or current. In a solution, the equilibrium concentrations of the reduced and oxidized forms of a redox couple are linked to the potential (E) via the *Nernst's Equation* **(Eq. 3.1)**:

$$E = E_0 + \frac{RT}{nF} \ln \frac{Coxi}{Cred} \qquad 3.1)$$

3.10.2.1) Cyclic Voltammetry

Cyclic voltammetry is the study of current variations over a range of electrode potentials (potential window). The same potential window is then scanned in the reverse direction (hence the term cyclic). The plot of current versus voltage of the electrode potential hence obtained is a cyclic voltammogram (CV). Electroactive species formed by oxidation on the forward scan can be reduced on the reverse scan if the reaction is reversible. It is used to study the electrochemical properties of substances in both in solution state as well as at the electrode/electrolyte interface. Information regarding the cathodic and anodic peak potential (Epc; Epa) and the cathodic and anodic peak current (Ipc, Ipa) can be obtained. CV can also determine the electrode potentials required for the oxidation or reduction of different redox species (e.g. mediators). This involves cycling a mediator solution between two fixed potentials versus Ag/AgCl at a desired scan rate. During oxidation and reduction, the mediator shows a peak on the cyclic voltammogram, depending on whether the redox reaction is reversible. The determined peak potential can be used as working potential during e.g. amperometric measurements [Evans *et al*., 1983; Kissinger *et al.*, 1983].

3.10.3) X-ray diffraction (XRD)

XRD studies were conducted on a Bruker D-8 Advance diffractometer. A monochromatic X-ray beam with Cu-Kα radiation (λ = 1.5406 Å) has been used to record the spectrum. XRD works on constructive interference of monochromatic X-rays on a crystalline sample. The cathode ray tube generates X-rays which are further filtered and collimated to produce monochromatic radiation and concentrate, and made to fall onto the sample. Upon meeting the conditions of Braggs Law (**Eq. 3.2**), this interaction between the sample and incident ray produces constructive interference patterns and a diffracted ray

$$2d \sin\theta = n\lambda \quad \text{.....3.2)}$$

Where, λ = wavelength of electromagnetic radiation, θ = diffraction angle and d = lattice spacing in a crystalline sample. These diffracted X-rays then need to be detected, processed and counted. The lattice with all possible diffraction directions is attained by scanning the sample through a range of 2θ angles due to the random orientation of the powdered material. This technique is used to characterize the crystallographic structure, crystallite size (grain size) and preferred orientation in polycrystalline or powder solid samples.

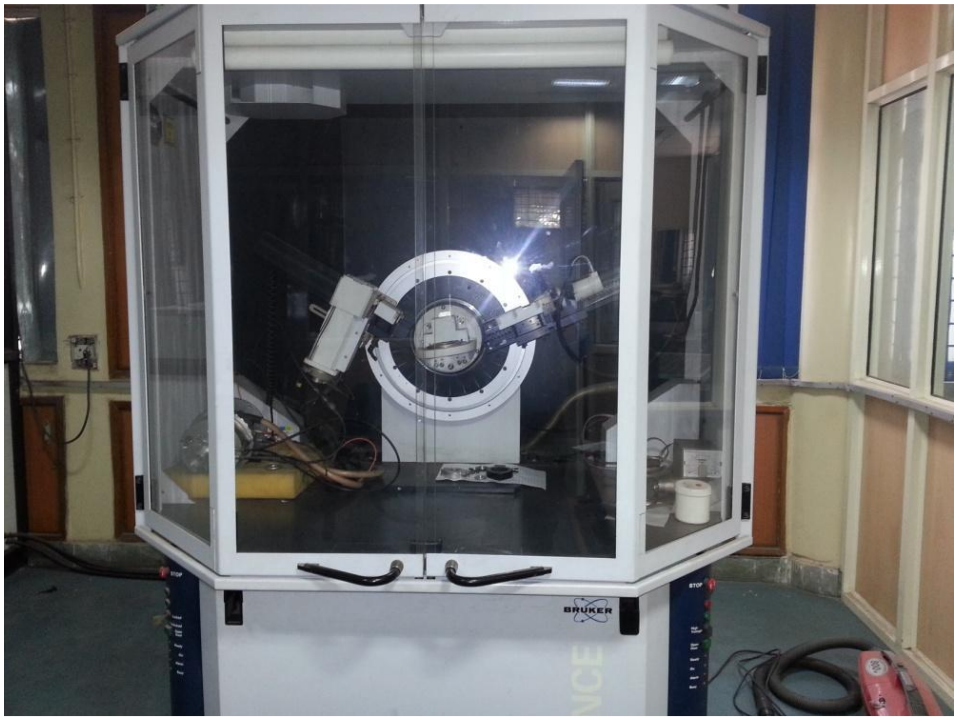

Fig 3.8: X-ray diffractometer (Bruker N8 Advance).

The mean size of the nanoparticles can also be determined from the peak broadening in the X-ray diffraction pattern by using Debye– Scherrer equation **(Eq. 3.3):**

$$D = \frac{0.9\lambda}{\beta Cos\theta} \quad \text{.....3.3)}$$

where, D = average crystallite size (Å), λ = wavelength of X-rays (Cu Kα: λ = 1.5418 Å), θ = Bragg diffraction angle, and β = full width at half maximum (in radians).

3.10.4) Scanning electron microscopy (SEM)

SEM analysis has been carried out to determine the morphology of the fabricated paper disc (Hitachi S-3700N). This technique utilizes a beam of highly energetic electrons and can examine objects on a very fine scale. The electron beam is generated by a high energy source, e.g., heated tungsten, and scanned over a specimen. As the beam hits the sample, electrons and X-rays are ejected from the sample which is collected by detectors and processed to produce a visual image of the fine structure of the sample. The 10 nm resolution of SEM allows the visualization of materials at sub-micron levels.

Fig. 3.9: Scanning electron microscope (SEM; S-3700N).

3.10.5) Fourier transform infrared (FT-IR) spectroscopy

FT-IR spectroscopy of the synthesized nanoparticle was conducted on a Perkin-Elmer instrument. FT-IR is an analytical technique used for the structural characterization of organic materials. It is based on the specific infrared absorption displayed by molecular bonds depending upon their vibrational states. In the FT-IR spectra, the appearance or non-appearance of certain

vibrational frequencies gives valuable information about the structure of a particular molecule. Each functional group has a specific range of vibrational frequencies and is very sensitive to the chemical environment, thus providing valuable information regarding the presence of certain functional groups in the specific sample for their further characterization. FTIR spectrophotometer has a spectrum in the range of 400-4000 cm^{-1}.

Fig. 3.10: FTIR (Perkin Elmer)

3.10.6) <u>Contact angle (CA) measurement</u>

The angle at which a liquid/vapor interface meets a solid surface is the contact angle (CA). The CA is specific for any given system and is determined by the interactions across an interface. It depends upon surface roughness, surface condition and surface material. CA describes the shape of a liquid droplet resting on a solid surface. When a tangent line is drawn from a droplet to touch the solid surface, the angle between the tangent line and the solid surface is known as the contact angle. This technique is surface sensitive and can detect surface properties such as surface energy, wettability and adhesion. The measurements were carried out to investigate the

hydrophilic/hydrophobic character of the surface that can be correlated to material behaviour/deposition as well as the immobilization of the biomolecule onto the electrodes by a Sessile drop method. The Sessile drop method is used to estimate wetting properties of a localized region on a solid surface by measuring the angle between the baseline of the drop and the tangent at the drop boundary. When CA is less than 90°, the surface is known as hydrophilic, and if it is more than 90°, it is hydrophobic. If the angle is above ~150°, it is superhydrophobic, and if it is less than ~20°, it is super-hydrophilic.

Fig. 3.11: Contact angle

4) Results

4.1) Effect of hydrophilicity of PET substrate on electrochemical performance of SPEs

4.1.1) Contact angle

Contact angle (CA) measurements were conducted to investigate the hydrophobic/hydrophilic nature of the SPE. There are two important factors which need to be considered to guarantee appropriate printing precision and quality i.e. thermal stability and surface affinity of PET substrate. Ink adhesion can be genuinely influenced by hydrophilicity or hydrophobicity of PET substrate. [108] (Du, C. X., et al) Therefore, the contact angle of both the treated and untreated SPE was investigated As shown in the figure, CA values of water on untreated and treated SPE are found to be 73.36^0 and 23.48^0 respectively, demonstrating that the treated surface shows more hydrophilicity than the untreated surface.

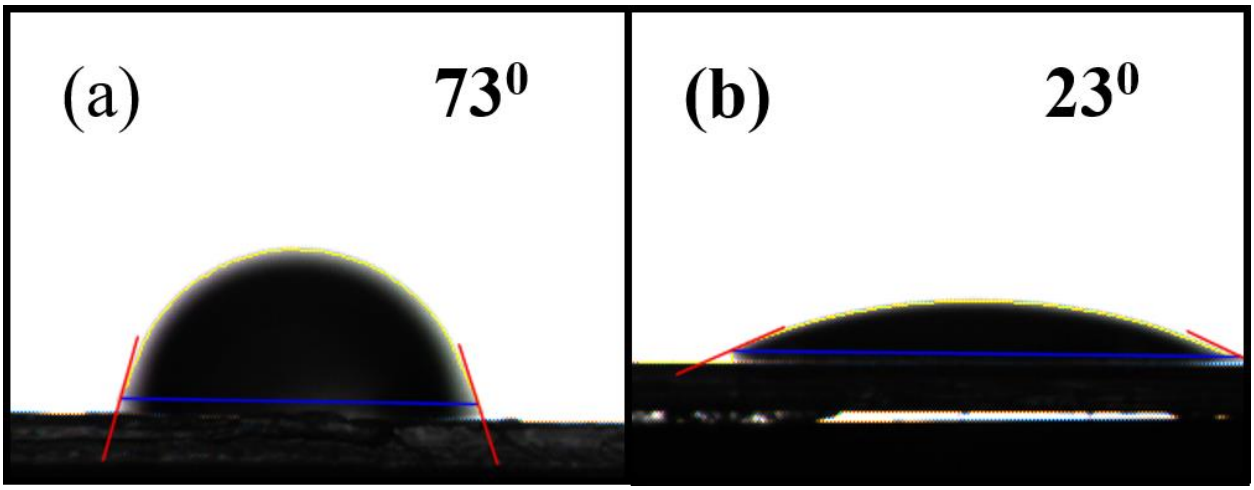

Figure 4.1: Contact angle of water on (A) Untreated (B) Treated SPE

4.2) Effect of pretreating procedures to SPEs

For enhancing the adhesion ability of graphite paste on PET substrate, insulating polymers were added, that results in enhanced charge transfer resistance that leads to a slower kinetics of the heterogeneous reaction along with quasi-reversible or irreversible redox processes. The principle

reason of pre-treating SPE was to remove these insulating polymers and to enhance the surface roughness and functionalities. The electrochemical performance of SPE was altogether improved after treating it with 3 M NaOH. The CV curves of before and then afterwards treatment of SPE were plotted in the figure. From the fig. 4.2, the oxidation peak current of NaOH treated SPE was found to be higher than that of untreated SPE. This improvement may be ascribed to the removal of insulating binders from the surface of the working electrode.

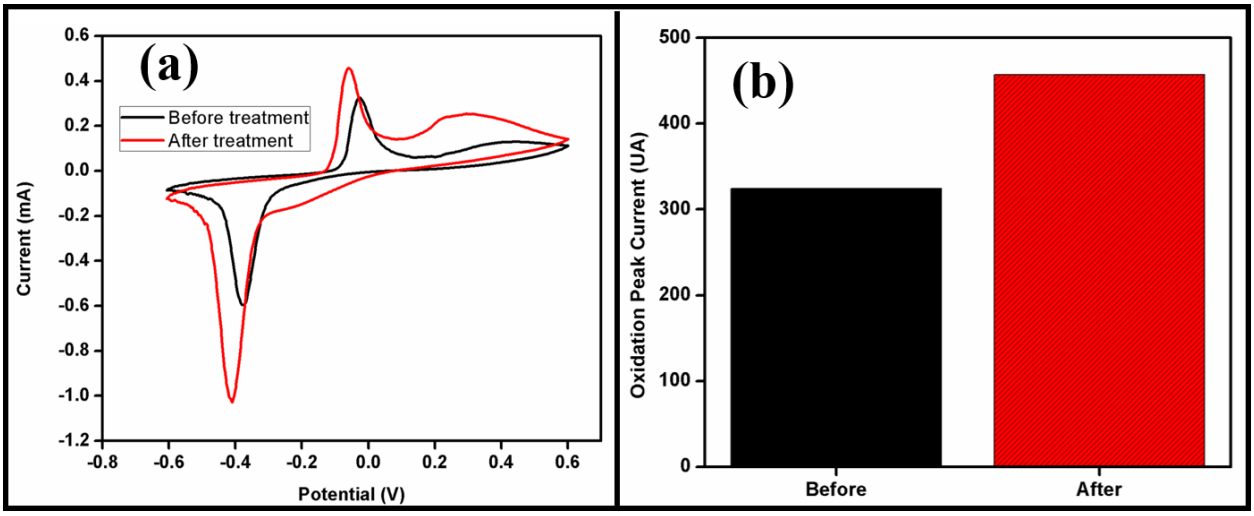

Fig 4.2: (a) Represents CV of SPEs before and after chemical treatment. (b) Oxidation peak current.

4.3) X-Ray Diffraction (XRD)

XRD pattern of the synthesized graphene oxide nanoparticles is shown in the fig. 4.3. Upon the oxidation of graphite, the 002 reflection peak shifted to a lower angle at $2\Theta = 11.2^0$ (d spacing = 0.79 nm) as compared to pristine graphite i.e. $2\Theta = 26.6^0$ (d spacing = 0.335 nm). This increase in d spacing can be due to the intercalation of water molecules and subsequent generation of oxygen functionalites in the interlayer spacing of graphite sheets [109].

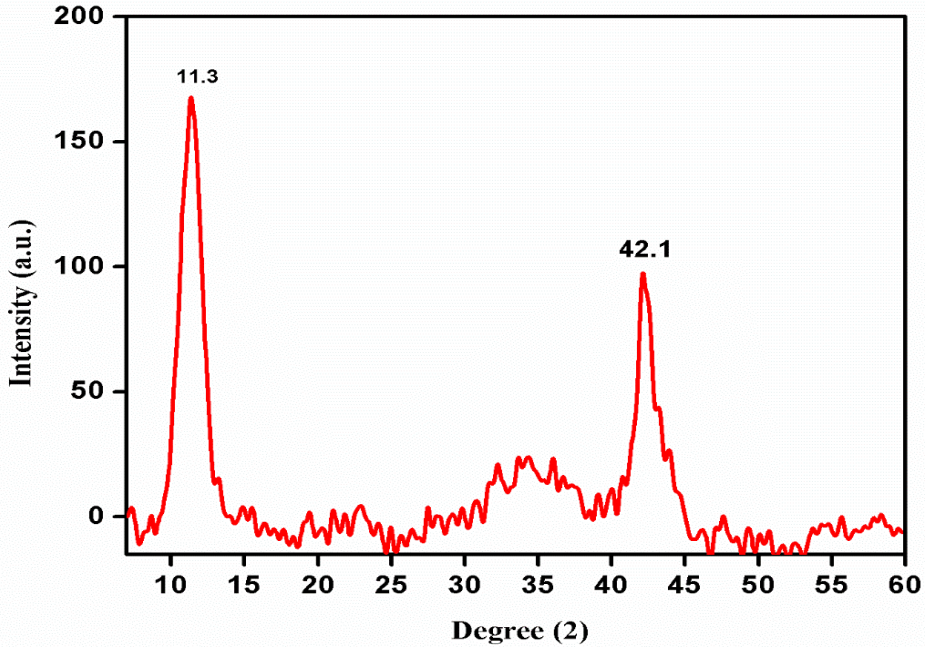

Fig 4.3: XRD of Graphene Oxide

4.4) Fourier transform infrared spectroscopy (FT-IR)

Fig. 4.4 shows FT-IR spectra of Graphene Oxide nanoparticle in the range of 500-4000 cm^{-1} In this case, FT-IR spectrum shows a broad peak at 3000-3800 cm^{-1} which is attributed to O-H stretching vibration in GO which verifies the presence of the hydroxyl groups. The bands at 1730 and 1400 cm^{-1} are due to C=O stretching and O-H bending vibrations of the carboxyl groups present in GO. The band appearing at 1627 cm^{-1} is due to the C=C stretching vibration, while the bands appearing at (1000-1280 cm^{-1}) are of ethers or epoxide groups [110].

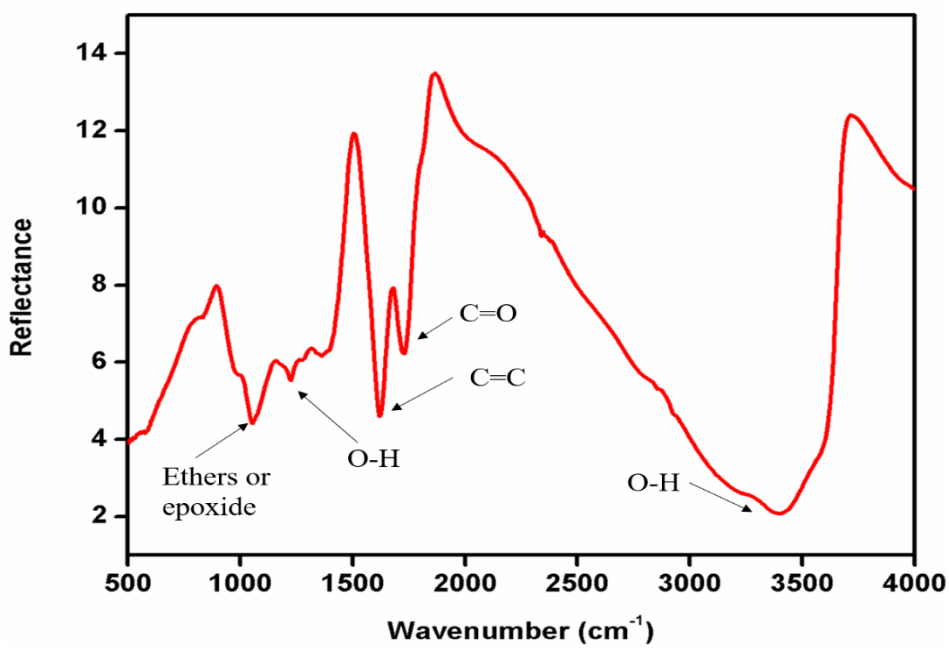

Fig 4.4: FTIR spectra of Graphene Oxide nanoparticle.

4.5) <u>UV</u>

The UV-vis spectroscopic studies of GO were performed in a wavelength range 200-600 nm shown in fig. 4.5 which gives the general idea about the formation of graphene oxide. It was observed that the absorption increases consistently from 350 nm with maximum absorption occurring at 220 nm, due to $\pi - \pi^*$ transition of the aromatic C-C bonds of GO. The transparency of GO is much higher than that of the graphene.

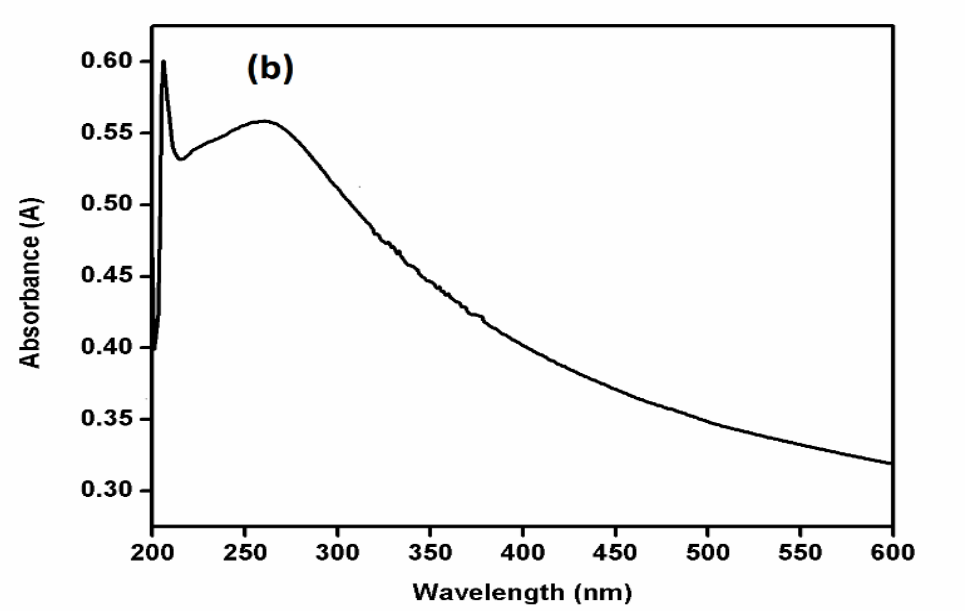

Fig 4.5: UV-visible spectrum of the AuNPs showing the characteristic absorption peak at 220 nm.

4.6) Scanning electron microscopy (SEM)

The surface morphologies of differently modified paper discs were examined by using scanning electron microscopy (SEM) shown in fig. 4.6. Image (a) shows SEM of Whatman paper where the cellulose fibrous structure is clearly visible, whereas fig (b) shows a SEM of GO modified paper, the stacks of graphene sheets were uniformly adsorbed between the cellulose fibres of Whatman paper. The SEM image of GO modified paper showed a smooth surface which indicated deposition of GO onto the Whatman paper. Fig (c) shows SEM of GO-GOx biocomposite on Whatman filter paper. It can be clearly seen that the morphology of the paper disc again changes which attributes to the presence of GOx layer which typically covered the surface of the matrix.

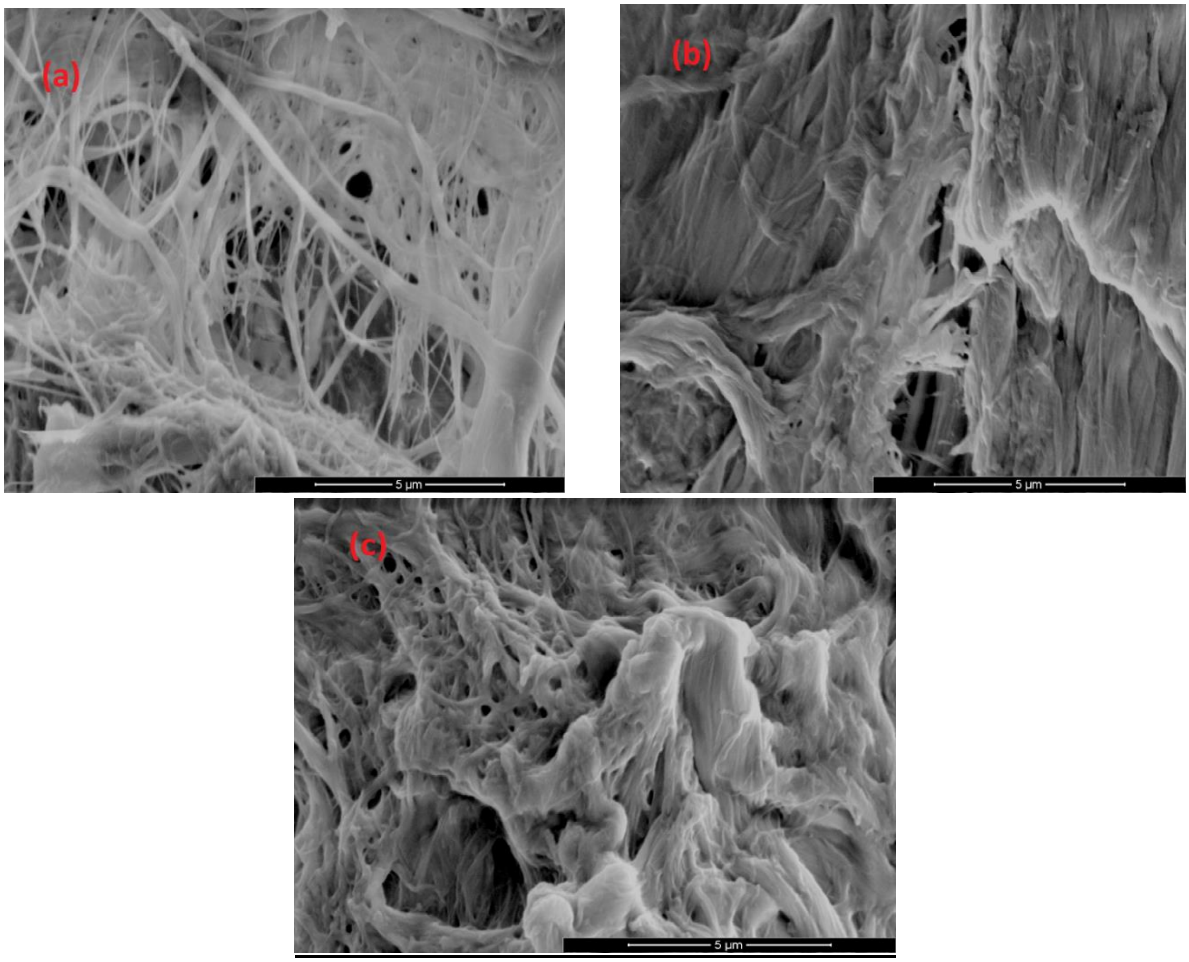

Fig 4.6: SEM micrographs (a) Whatman paper (b) GO on paper disc (c) GO-GOx on paper disc.

4.7) Electrochemical studies

Prior to performing the electrochemical measurement of glucose, we have optimised the experimental parameters such as the concentration of the nanomaterial, pH, ionic strength of the mediator and scan rate study. An optimization of each parameter was conducted by changing only a single parameter, while the other parameters remained constant.

4.7.1) GO Concentration

Fig. 4.7 (a) depicts the cyclic voltammograms (CV) for oxidation of H_2O_2 recorded at (a) PEDOT: PSS (black) and (b) GO (red) modified paper disc on SPE in 0.1 M PBS containing 5 ×

10^{-3} M $[Fe(CN)_6]^{3-/4-}$ and 0.9% NaCl at a scan rate of 50 mVs^{-1}. As it is clearly visible, the GO modified paper disc on SPE shows much favourable electrochemical activities towards the catalysis of H_2O_2. While there is no observable oxidation peak in case of PEDOT: PSS modified paper disc on SPE. Therefore the figure reveals the use of GO modified paper disc increases the charge transfer leading to an enhanced signal response in comparison to PEDOT: PSS modified paper disc.

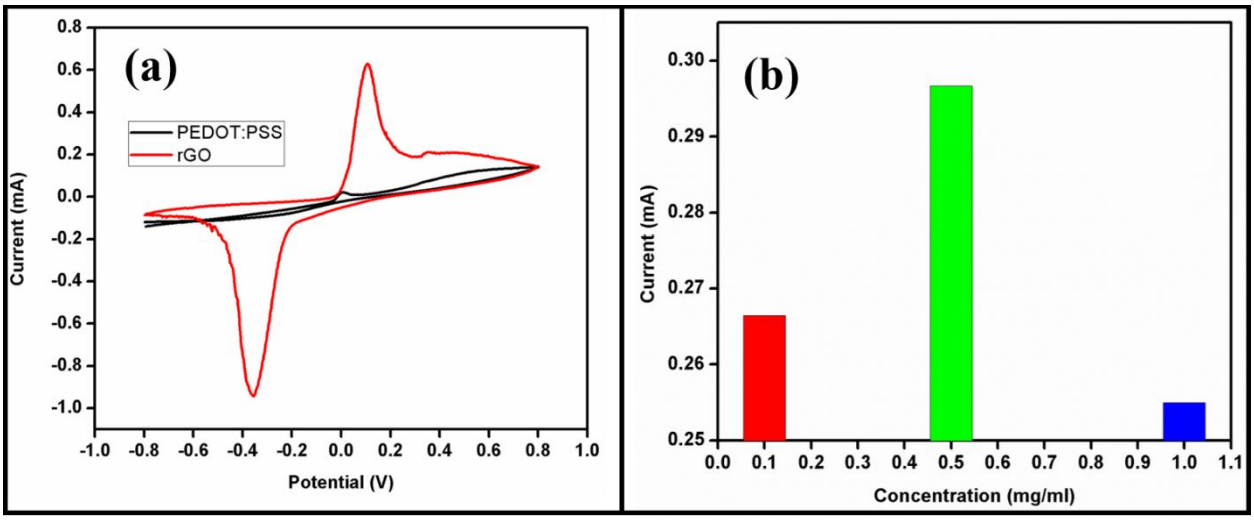

Fig 4.7: (a) CV of paper disc modified with different material in 0.1 M PBS pH 7.0 at a scan rate of 50 mV/s i) PEDOT: PSS ii) GO and (b) Current response of the different concentrations of GO in composite i.e. 0.1, 0.5, 1 mg/ml.

Figure 4.7 (b) depicts the optimization of GO concentration in a biocomposite. We can clearly see the variation in the electrochemical response with the different concentration of GO in a biocomposite. It was observed that the GO concentration, i.e., 0.5 mg/ml exhibiting the maximum current response. Therefore, to conduct further electrochemical experiments we opted 0.5 mg/ml concentration of GO in a biocomposite.

4.7.2) pH study

The pH optimization is a key element because the amino acids which are present at the active sites of the enzyme depend upon electrostatic interaction to combine with a substrate which in turn relies on pH of the solution. It can be stated that the sensitivity of the biosensor is influenced by the pH of the electrolyte because the bioactivity of GOx is pH dependent. The effect of pH on the fabricated GO-GOx paper disc has been examined using CV at a scan rate of 50 mVs^{-1} in 0.1 M PBS containing 5 mM $[Fe(CN)_6]^{3-/4-}$ and 0.9% NaCl.

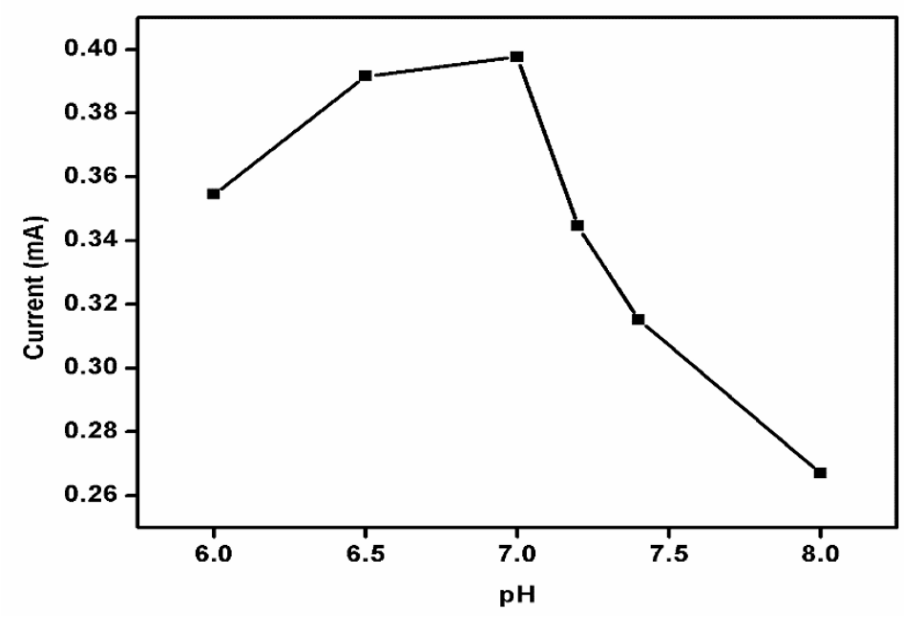

Fig 4.8: Current response of rGO-GOx/paper electrode as a function of pH.

The paper based biosensor gives an optimum response at pH 7.0 over a pH range 6.0 to 8.0. Fig. 4.8 indicate that magnitude of current response is maximum at pH 7 which attribute the fact that at neutral pH the biomolecules such as an antibody, enzymes, amino acid etc. are present in their natural form with maximum efficacy and the stability whereas these biomolecules get denatured in the acidic as well as basic medium. [111] (kumar. et al) Subsequently, all the further experiments have been performed at pH 7.0 so that the biomolecules keep up its characteristic structure.

4.7.3) Ionic strength study

The biosensor response to glucose in PBS (pH 7.0) was analyzed with the different concentrations of PBS ranging from 25-200 mM shown in fig. 4.9. The current response of the electrode increased steadily with increasing concentration of PBS (from 25 to 100 mM) with the most significant increase obtained at 100 mM. At low PBS concentration, the response was limited by the enzyme-mediator kinetics, whereas at high PBS concentration, the response was limited by enzyme-substrate kinetics. A higher concentration beyond 100 mM provided very noisy signal and this could be caused by saturation of the mediator solubility in buffer solution.

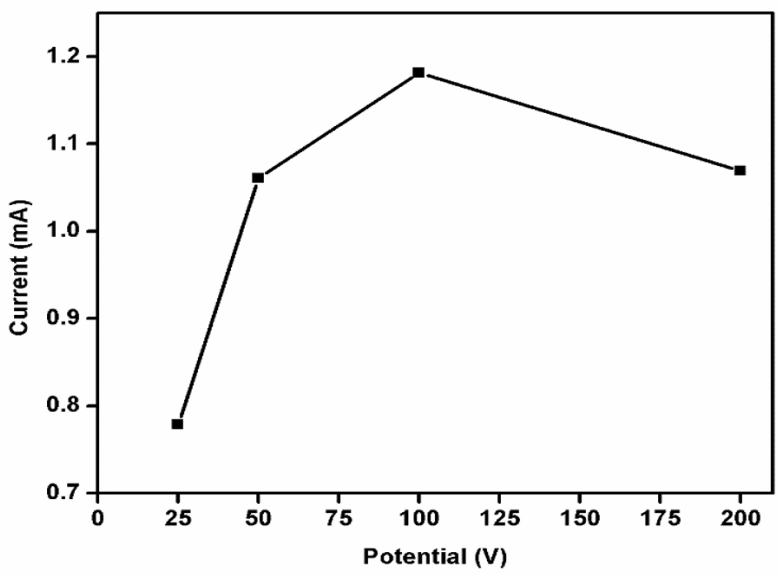

Fig 4.9: Current response of enzyme electrode at different Ionic strength i.e.25 mM, 50 mM, 100 mM & 200 mM

4.7.4) Scan rate study

Fig 4.10 and 4.11 show CV response of rGO/paper and rGO-GOx/paper electrode as a function of scan rate (10–100 mVs^{-1}) respectively. We observe that both cathodic (I_{pc}) and anodic (I_{pa}) peak current vary linearly with square root of the scan rate (insets a) in Figures 4.10 and 4.11,

indicating that electrochemical reaction is a diffusion-controlled process. The slopes and intercepts are given by Eq (4.1) – (4.4)

$$I_{pa(rGO/paper)} = [0.16\ \mu A(smV^{-1})\ \times \left(scan\ rate[mVs^{-1}]\right)^{1/2}] - 0.27\mu A, R^2\ =\ 0.98\ldots..4.1)$$

$$I_{pc(rGO/paper)} = [(-0.18)\mu A(smV^{-1})\ \times \left(scan\ rate[mVs^{-1}]\right)^{1/2}] - 0.28\ \mu A, R^2\ = 0.99..4.2)$$

$$I_{pa(rGO-GOx/paper)} = [0.17\ \mu A(smV^{-1})\ \times \left(scan\ rate[mVs^{-1}]\right)^{1/2}] - 0.13\ \mu A, R^2\ =$$

0.99….4.3)

$$I_{pc(rGO-GOx/paper)} = [(-0.19)\mu A(smV^{-1})\ \times \left(scan\ rate[mVs^{-1}]\right)^{1/2}] - 0.26\ \mu A, R^2 =$$

0.99…..4.4)

The difference of cathodic (E_{pc}) and anodic (E_{pa}) peak potentials ($\Delta E_p = E_{pc} - E_{pa}$) and square root of scan rate for rGO/paper and rGO-GOx/paper electrodes exhibit a linear relationship and are given by eq. (4.5) and (4.6). A good linear fitting suggests a facile electron transfer from medium to electrode.

$$\Delta E_p(V)_{rGO/paper} = [0.01198\ A(smV^{-1})\ \times \left(scan\ rate[mVs^{-1}]\right)^{1/2}] + 0.2274\ A, R^2\ =$$

0.99...4.5)

$$\Delta E_p(V)_{rGO-GOx/paper} = [0.01115\ A(smV^{-1})\ \times \left(scan\ rate[mVs^{-1}]\right)^{1/2}] + 0.2218\ A, R^2\ =$$

0.99…….4.6)

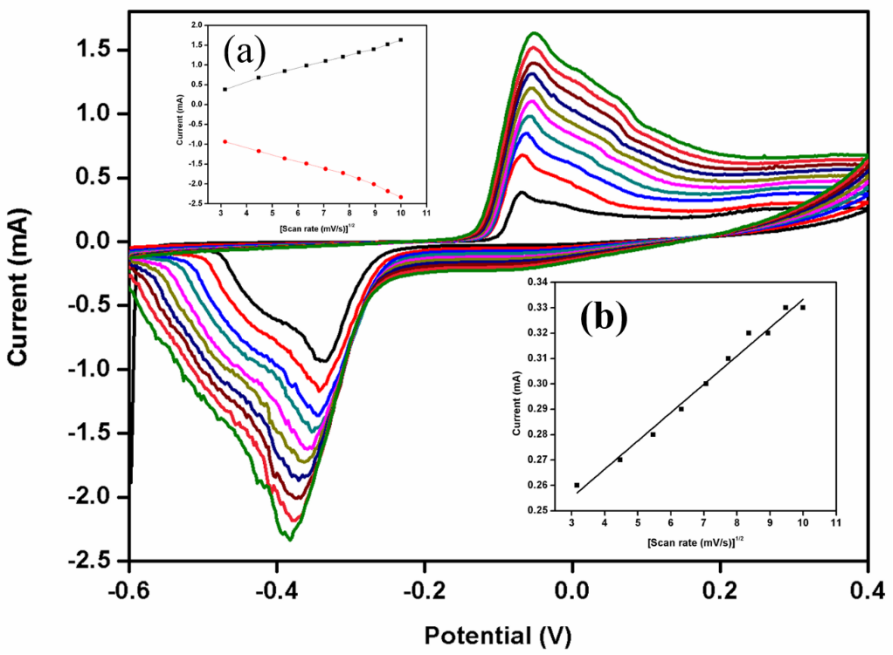

Fig 4.10: Cyclic voltammetry (CV) of rGO/paper electrode as a function of scan rate 10-100 (mV/s). Magnitude of oxidation and reduction current response as a function of square root of scan rate (mV/s) (inset a), and difference of cathodic and anodic peak potential (ΔEp) as a function of square root of scan rate (inset b).

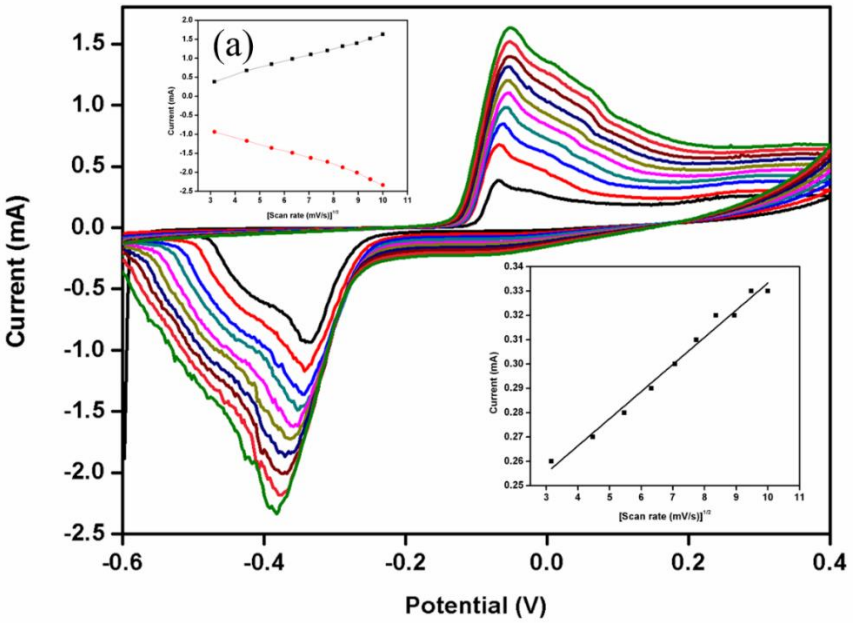

Fig 4.11: Cyclic voltammetry (CV) of rGO-GOx/paper electrode as a function of scan rate 10-100 (mV/s). Magnitude of oxidation and reduction current response as a function of square root of scan rate (mV/s) (inset a), and difference of cathodic and anodic peak potential (ΔEp) as a function of square root of scan rate (inset b).

Upon the completion of various optimization parameters, we draw our conclusion of the parameters on the performance of the biosensor. It is suggested using 0.1 M PBS (pH 7.0) as a mediator solution with a scan rate of 50 mVs^{-1} and the optimized concentration of GO in a composite is 0.5 mg/ml for the determination of glucose samples.

4.8) Reduction of GO to rGO by Electrochemical method

The CV of electrochemical reduction process of the GO on SPE equipped with paper disc is shown in the Fig. 4.12. GO has many functional moieties such as hydroxyl, carboxylic acid, quinine, ketone, etc. When the enzyme GOx is dispersed in the GO solution, the functional groups in GO can bind covalently with the free amino groups of GOx. Consequently, we can state that GOx is immobilized by both entrapment and covalent binding. This prepared GO-GOx composite was reduced electrochemically by providing a specific number of cycles and potential range. The figure indicates that in first cycle, a broad cathodic peak (Ipc) with an onset potential of -0.4 V was obtained, indicating that oxygen containing functionalities of GO has been reduced. After this in the consecutive cycles, a significant decrease in the reduction current. The modified electrode is represented as rGO-GOx paper disc/SPE. [112]

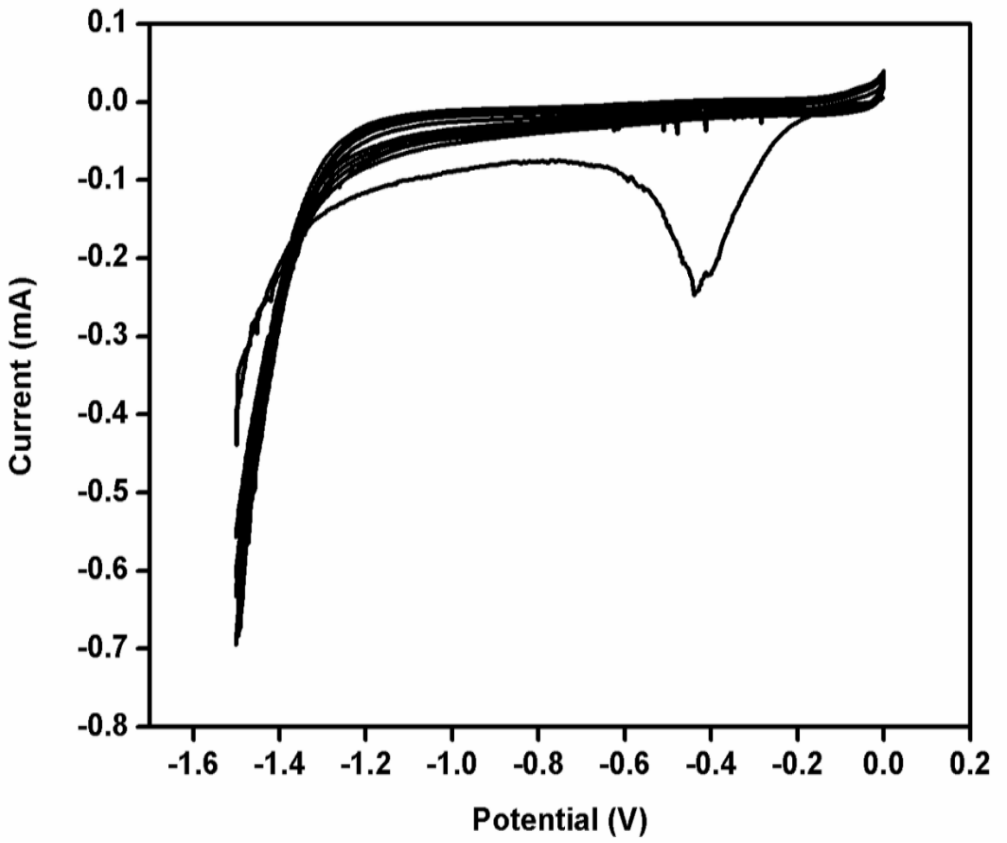

Fig 4.12: CV of electrochemical reduction of GO-GOx to rGO-GOx on paper disc in 0.1 M PBS (pH 7.0) at a scan rate of 50 mVs^{-1}.

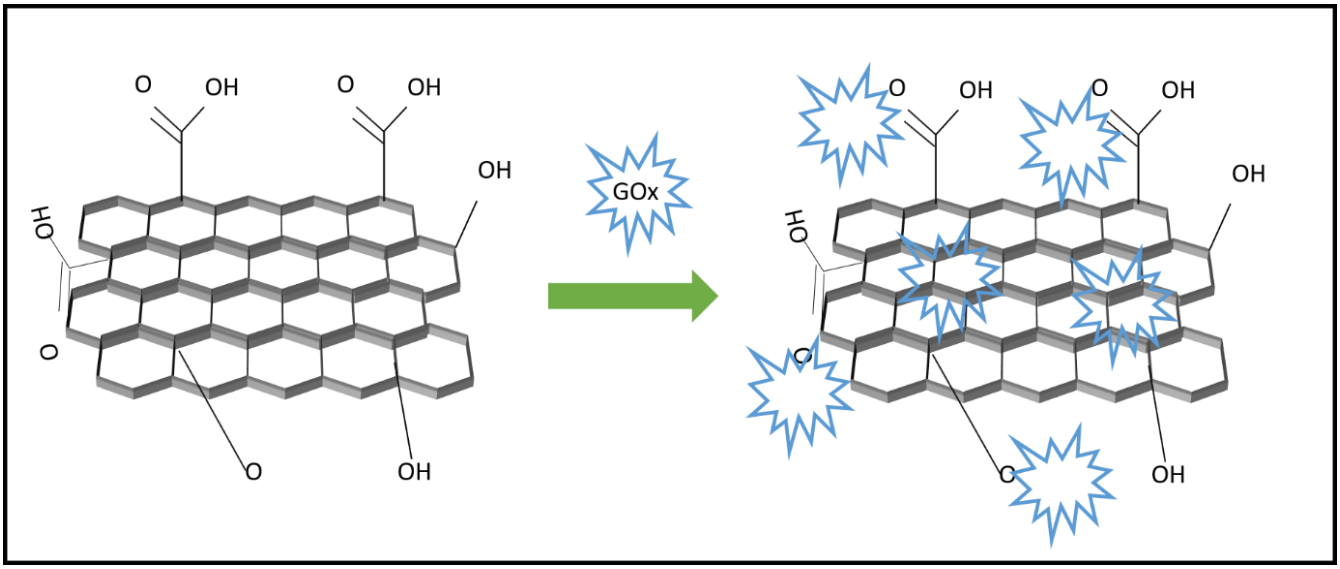

Fig. 4.13: Schematic representation of covalent binding of GO-GOx.

4.9) Electrode studies

The charge transfer phenomenon has been investigated at the electrode/solution interface after different surface modification of paper disc by using the Electrochemical Impedance Spectroscopy (EIS) technique. The charge transfer resistance (Rct) at the electrode/solution interface can be evaluated by using the diameter of semicircle in Nyquist plot.

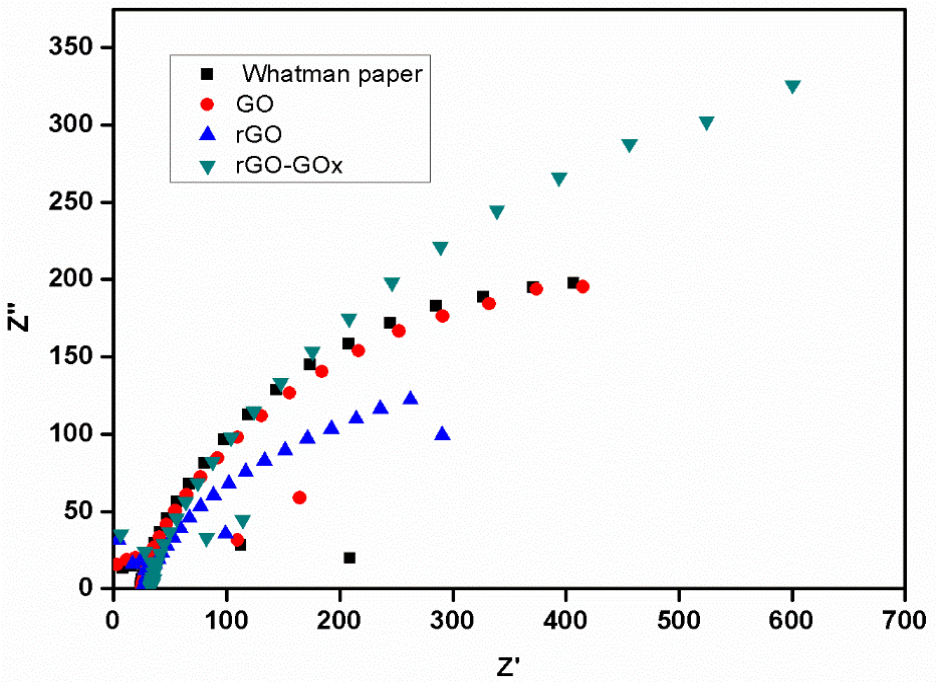

Fig 4.14: Electrochemical Impedance Spectroscopy (EIS) of a) whatman paper, b) GO/paper c) rGO/paper, and d) rGO-GOx/paper electrodes.

Fig. 4.14 indicate the Rct of bare whatman paper was found to be 613 Ω. After incorporation of GO, the Rct reduced to 483 Ω. The modified surface can be corelated with the charge transfer resistance confirming deposition of GO over paper disc. After electrochemical reduction of GO to rGO, the Rct of rGO further reduced to 370.35 Ω. This increase in conductivity may be attributed to the formation of rGO. These results indicate that GO has been electrochemically reduced to rGO over paper disc and enhances the charge transfer from solution to electrode due to high conducting and electrochemical behavior of rGO which results in increase of the permeability of

$[Fe(CN)6]^{3-/4-}$ to the surface of rGO/paper electrode. After GOx immobilization the Rct increased to 734.2 Ω this may be attributed to the insulating behaviour of the glucose oxidase that further hinders the tranfer of electron from the electrolyte to the electrode surface.

*4.10) **Response studies***

The electrochemical response of rGO-GOx bioelectrode has been measured as a function of glucose concentration (50-500 mg/dl) in 0.1 M PBS (pH 7.0, 0.9% NaCl) containing [5 mM $Fe(CN)_6$ $]^{3-/4-}$ at scan rate of 50 mVs^{-1} using the Cyclic Voltammetry (CV) technique (Fig. 4.15). The biochemical reaction **(Scheme)** involved in the measurement is:

$$\text{Glucose} + \text{GOx–FAD}^{+} \longrightarrow \text{Gluconolactone} + \text{GOx–FADH}_2 \qquad \text{(i)}$$

$$\text{GOx–FADH}_2 + O_2 \longrightarrow \text{GOx–FAD} + H_2O_2 \qquad \text{(ii)}$$

$$H_2O_2 \longrightarrow 2H^{+} + O_2 + 2\,e^{-} \qquad \text{(iii)}$$

The electrochemical response of the rGO-GOx film towards the oxidation of glucose has been carried out by observing proportional O_2 consumption in PBS with the increasing glucose concentration. During the oxidation of glucose, FAD accepts electrons from glucose to reduce to $FADH_2$ which further reacts with O_2 to form FAD and H_2O_2. The figure displays the cyclic voltammogram of rGO–GOx in PBS at various glucose concentrations. The increase in the oxidation peak current as the function of glucose concentration indicates an increase in H_2O_2 concentration. The calibration curve using glucose standard shows a linear response from the rGO-GOx electrode in the concentration range of 50-500 mg/dl in fig. 4.15 (b) with a regression coefficient of 0.99 as given by the following eq:

Ip = [0.33 µAdl/mg) × (conc. of glucose (mg/dl))] + 0.592 mA, $R^2 = 0.99$. ……4.7)

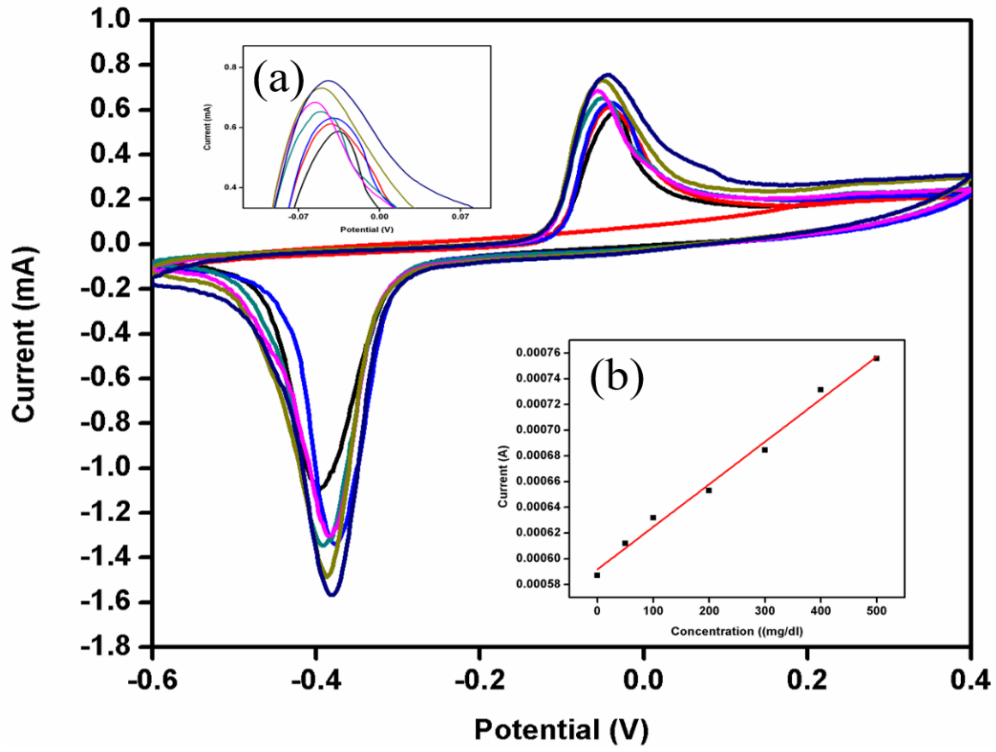

Fig 4.15: The electrochemical response of rGO-GOx/paper disc as a function of glucose concentration (mg/dl). (inset a) The magnified image of oxidation peak current, (inset b) calibration curve between magnitude of peak current and glucose concentration (mg/dl).

The sensitivity of the rGO-GOx electrode has been estimated to be 0.33 µAdl/mg and the lower detection limit has been found to be as 0.126 mg/dl by using the equation (4.8)

$$\text{Detection limit} = 3\sigma/m \qquad \ldots\ldots\ldots 4.8)$$

Where σ = standard deviation and m = slope of the curve.

4.11) Interferent study

For determining the selectivity of the rGO-GOx bioelectrode, we have performed the interferent study by measuring the electrochemical response upon the addition of different interferents present in serum (fig. 4.16). The potential interferents used in this study are lactic acid (0.5 mM), uric acid (0.1 mM), , and ascorbic acid (0.05 mM) and urea (1mM) in phosphate buffer (0.1 M, pH 7, 0.9% NaCl) containing 5 mM $[Fe(CN)_6]^{3-/4-}$. The oxidation peak current in the electrochemical response studies shows that the current value increases by a negligible amount.

The values obtained for the oxidation current in the electrode in the presence of glucose, lactic acid, uric acid, urea, uric acid, lactic acid, and ascorbic acid is 1.12, 1.23, 1.406, and 1.22 respectively, indicating the high selectivity of electrode towards glucose.

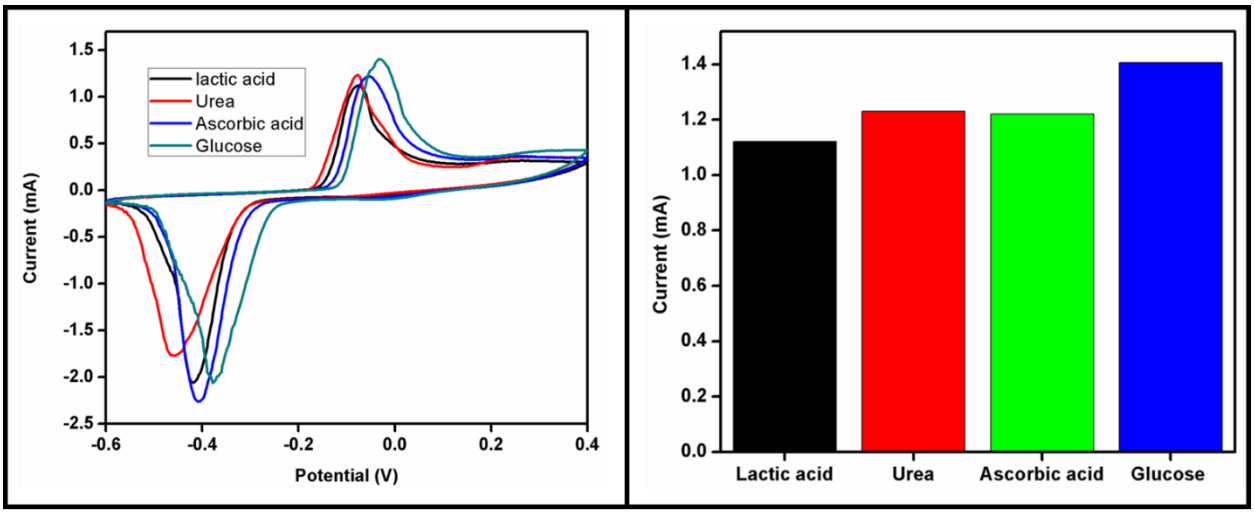

Fig 4.16: Interferent studies of rGO-GOx/paper electrode.

5) Conclusion

A miniaturized, low cost, portable and disposable amperometric biosensor used for glucose concentration detection was developed by using cellulose paper as an immobilizing matrix for the biocomposite via a simple adsorption step. The optimised conditions were systematically studied for the operation and development of biosensor. For the preparation of rGO-GOx composite, a single step electrochemical method has been used. The coupling of modified paper disc with SPE allowed the determination of glucose with low-cost, lower volumes of samples and reagents.and shorter assay time detection device as compared with the traditional techniques. The developed biosensor exhibits good linear range and storage stability. While our work was simply focused on the detection of glucose, we believe that the possibilities of further manipulation of paper based enzyme immobilization which can be integrated with various (bio)chemical systems toward the development of simplified point-of-care applications could be further explored.

6) Future Perspective

The result of experiment have revealed that the rGO-GOx platform can efficiently be utilized in the development of sensitive and high performance electrochemical biosensing device for both laboratory and point of care application. Besides this application, studies should be carried out to explore other applications of this platform. This platform can be integrated with microfluidic device which would further open a new area of research and probably meet the real challenge in high performance biosensor

*7) **References***

1. Srivastava, Saurabh, et al. "Electrophoretically deposited reduced graphene oxide platform for food toxin detection." *Nanoscale* 5.7 (2013): 3043-3051.
2. Karuwan, Chanpen, et al. "A disposable screen printed graphene–carbon paste electrode and its application in electrochemical sensing." *RSC Advances* 3.48 (2013): 25792-25799.
3. Kumar, Suveen, et al. "Biofunctionalized nanostructured zirconia for biomedical application: a smart approach for oral cancer detection." *Advanced Science* 2.8 (2015).
4. Morrin, Aoife, Anthony J. Killard, and Malcolm R. Smyth. "Electrochemical characterization of commercial and home-made screen-printed carbon electrodes." *Analytical Letters* 36.9 (2003): 2021-2039.Kadara, Rashid O., Norman Jenkinson, and Craig E. Banks. "Characterisation of commercially available electrochemical sensing platforms." *Sensors and Actuators B: Chemical* 138.2 (2009): 556-562
5. Fanjul-Bolado, Pablo, et al. "Electrochemical characterization of screen-printed and conventional carbon paste electrodes." *Electrochimica Acta*53.10 (2008): 3635-3642.
6. Couto, R. A. S., J. L. F. C. Lima, and M. B. Quinaz. "Recent developments, characteristics and potential applications of screen-printed electrodes in pharmaceutical and biological analysis." *Talanta* 146 (2016): 801-814.
7. Rungsawang, Tipawan, et al. "Development of Electrochemical Paper-based Glucose Sensor Using Cellulose-4-aminophenylboronic Acid-modified Screen-printed Carbon Electrode." *Electroanalysis* 28.3 (2016): 462-468.
8. Rama, Estefanía Costa, and Agustín Costa-García. "Screen-printed Electrochemical Immunosensors for the Detection of Cancer and Cardiovascular Biomarkers." *Electroanalysis* 28.8 (2016): 1700-1715.
9. Banks, Craig E., Christopher W. Foster, and Rashid O. Kadara. *Screen-Printing Electrochemical Architectures*. Springer, 2015.
10. Laschi, S., et al. "Development of disposable low density screen-printed electrode arrays for simultaneous electrochemical measurements of the hybridisation reaction." *Journal of Electroanalytical Chemistry* 593.1 (2006): 211-218.
11. Tan, Swee Ngin, Liya Ge, and Wei Wang. "Paper disk on screen printed electrode for one-step sensing with an internal standard." *Analytical chemistry* 82.21 (2010): 8844-8847.

12. de Mattos, Ivanildo Luiz, Lo Gorton, and Tautgirdas Ruzgas. "Sensor and biosensor based on Prussian Blue modified gold and platinum screen printed electrodes." *Biosensors and Bioelectronics* 18.2 (2003): 193-200.
13. Honeychurch, Kevin C., and John P. Hart. "Screen-printed electrochemical sensors for monitoring metal pollutants." *TrAC Trends in Analytical Chemistry*22.7 (2003): 456-469.
14. Ping, Jianfeng, et al. "Simultaneous determination of ascorbic acid, dopamine and uric acid using high-performance screen-printed graphene electrode." *Biosensors and Bioelectronics* 34.1 (2012): 70-76.
15.
16. Ho Yang, Min, et al. "Directed Self-Assembly of Gold Nanoparticles on Graphene-Ionic Liquid Hybrid for Enhancing Electrocatalytic Activity." *Electroanalysis* 23.4 (2011): 850-857.
17. Wang, Kun, et al. "Enhanced direct electrochemistry of glucose oxidase and biosensing for glucose via synergy effect of graphene and CdS nanocrystals." *Biosensors and Bioelectronics* 26.5 (2011): 2252-2257.
18. Kumar, Saurabh, et al. "Conducting paper based sensor for cancer biomarker detection." *Journal of Physics: Conference Series*. Vol. 704. No. 1. IOP Publishing, 2016.00\03
19. Tan, Swee Ngin, et al. "based enzyme immobilization for flow injection electrochemical biosensor integrated with reagent-loaded cartridge toward portable modular device." *Analytical chemistry* 84.22 (2012): 10071-10076.
20. Wu, Yafeng, et al. "A paper-based microfluidic electrochemical immunodevice integrated with amplification-by-polymerization for the ultrasensitive multiplexed detection of cancer biomarkers." *Biosensors and Bioelectronics*52 (2014): 180-187.
21. Martinez, Andres W., et al. "Diagnostics for the developing world: microfluidic paper-based analytical devices." (2009): 3-10.
22. Wu, Yafeng, et al. "A paper-based microfluidic electrochemical immunodevice integrated with amplification-by-polymerization for the ultrasensitive multiplexed detection of cancer biomarkers." *Biosensors and Bioelectronics*52 (2014): 180-187.

23. Unnikrishnan, Binesh, Selvakumar Palanisamy, and Shen-Ming Chen. "A simple electrochemical approach to fabricate a glucose biosensor based on graphene–glucose oxidase biocomposite." *Biosensors and Bioelectronics*39.1 (2013): 70-75.
24. Kumar, Saurabh, et al. "Reduced graphene oxide modified smart conducting paper for cancer biosensor." *Biosensors and Bioelectronics* 73 (2015): 114-122.
25. Wu, Shixin, et al. "Graphene-based electrochemical sensors." *Small* 9.8 (2013): 1160-1172.
26. Kang, Xinhuang, et al. "Glucose oxidase–graphene–chitosan modified electrode for direct electrochemistry and glucose sensing." *Biosensors and Bioelectronics* 25.4 (2009): 901-905.
27. Liang, Bo, et al. "Study of direct electron transfer and enzyme activity of glucose oxidase on graphene surface." *Electrochemistry Communications* 50 (2015)
28. *World Health Organization*. Diabetes 2009 [cited 2010 01.09.2010]; Available from: www.who.int.]
29. King, Hilary, and Marian Rewers. "Diabetes in adults is now a Third World problem. The WHO Ad Hoc Diabetes Reporting Group." *Bulletin of the World health Organization* 69.6 (1991): 643
30. Krushinitskaya, Olga. *Osmotic sensor for blood glucose monitoring applications*. Diss. Vestfold University College, 2012
31. http://www.who.int/mediacentre/factsheets/fs312/en/
32. Non-Invasive Glucose Monitoring Techniques: A review and current trends
33. Non-Invasive Continuous Glucose Monitoring:Identi_cation of Models for Multi-Sensor Systems
34. S.N. Davis and G. Lastra-Gonzalez. Diabetes and Low Blood Sugar (Hypoglycemia). Journal of Clinical Endocrinology & Metabolism, 93(8), 2008.
35. Auxter, S. "Disease management models of diabetes take root." *Clinical Chemistry News* 8 (1996).
36. Free, Alfred H., and H. M. Free. "Self testing, an emerging component of clinical chemistry." *Clinical chemistry* 30.6 (1984): 829-838.
37. Wild, S., et al. "Global prevalence of diabetes: estimates for the year 2000 and projections for 2030 Diabetes Care 27: 1047–1053." *Find this article online* (2004).

38. Khalil, Omar S. "Non-invasive glucose measurement technologies: an update from 1999 to the dawn of the new millennium." *Diabetes technology & therapeutics* 6.5 (2004): 660-697.
39. Tura, Andrea, Alberto Maran, and Giovanni Pacini. "Non-invasive glucose monitoring: assessment of technologies and devices according to quantitative criteria." *Diabetes research and clinical practice* 77.1 (2007): 16-40.
40. Yeh, Shu-jen, et al. "Near-infrared thermo-optical response of the localized reflectance of intact diabetic and nondiabetic human skin." *Journal of biomedical optics* 8.3 (2003): 534-544.
41. Chang, Raymond. *Physical chemistry for the biosciences*. University Science Books, 2005.
42. H. S. Stoker, *Organic and Biological Chemistry*. Cengage Learning, (2012).
43. Koshland, Daniel E. "The key–lock theory and the induced fit theory." *Angewandte Chemie International Edition in English* 33.23-24 (1995): 2375-2378.
44. Sekretaryova, Alina. *Novel reagentless electrodes for biosensing*. Vol. 1689. Linköping University Electronic Press, 2014.
45. Heurich, Meike. "Development of an affinity sensor for ochratoxin A." (2008).
46. Clark, Leland C., and Champ Lyons. "Electrode systems for continuous monitoring in cardiovascular surgery." *Annals of the New York Academy of sciences* 102.1 (1962): 29-45.
47. Kaushik, Ajeet, et al. "Nano-biosensors to detect beta-amyloid for Alzheimer's disease management." *Biosensors and Bioelectronics* 80 (2016): 273-287.
48. Cortina, María E., et al. "Electrochemical magnetic microbeads-based biosensor for point-of-care serodiagnosis of infectious diseases." *Biosensors and Bioelectronics* 80 (2016): 24-33.
49. Gilmartin, Markas AT, and John P. Hart. "Novel, reagentless, amperometric biosensor for uric acid based on a chemically modified screen-printed carbon electrode coated with cellulose acetate and uricase." *Analyst* 119.5 (1994): 833-840.
50. Chaubey, Asha, and BlD Malhotra. "Mediated biosensors." *Biosensors and bioelectronics* 17.6 (2002): 441-456.

51. Ali, M. Ben, et al. "Formaldehyde assay by capacitance versus voltage and impedance measurements using bi-layer bio-recognition membrane." *Biosensors and Bioelectronics* 22.5 (2006): 575-581.
52. Ravichandran K, Baldwin RP (1981) J Electroanal Chem Interfacial Electrochem 126:293–300
53. Metters JP, Kadara RO, Banks CE (2011) Analyst 136:1067–1076
54. Honeychurch KC, Hart JP (2003) Trends Anal Chem 22:456–469.
55. Honeychurch KC, Crew A, Northall H, Radbourne S, Davies O, Newman S, Hart JP (2013) Talanta 116:300–307
56. Shih Y, Zen JM, Yang HH (2002) J Pharm Biomed Anal 29:827–833
57. Wang Y, Xu H, Zhang J, Li G (2008) Sensors (Basel, Switzerland) 8:2043–2081
58. Carrara S, Shumyantseva VV, Archakov AI, Samorì B (2008) Biosens Bioelectron 24:148–150
59. Wang J, Rivas G, Ozsoz M, Grant DH, Cai X, Parrado C (1997) Anal Chem 69:1457–1460
60. Ren R, Leng C, Zhang S (2010) Biosens Bioelectron 25:2089–2094
61. Liu J, Su B, Lagger G, Tacchini P, Girault HH (2006) Anal Chem 78:6879–6884
62. Wang J, Rivas G, Ozsoz M, Grant DH, Cai X, Parrado C (1997) Anal Chem 69:1457–1460
63. Taleat Z, Khoshroo A, Mazloum-Ardakani M (2014) Microchim Acta 181:865–891.
64. Liu J, Su B, Lagger G, Tacchini P, Girault HH (2006) Anal Chem 78:6879–6884
65. Wang J, Tian B, Nascimento VB, Angnes L (1998) Electrochim Acta 43:3459–3465
66. Metters JP, Tan F, Kadara RO, Banks CE (2012) Anal Methods 4:1272–1277
67. Metters JP, Kadara RO, Banks CE (2012) Analyst 137:896–902
68. Foster CW, Pillay J, Metters JP, Banks CE (2014) Sensors 14:21905–21922
69. Tiwari I, Singh M, Gupta M, Metters JP, Banks CE (2015) Anal Methods 7:2020–2027
70. Choudhry NA, Kadara RO, Jenkinson N, Banks CE (2010) Electrochem Commun 12:406–409
71. Salazara P, Martín M, O'Neill RD, Roche R, González-Mora JL (2012) ElectroanalChem 674:48–56
72. Matemadombo F, Apetrei C, Nyokong T, Rodríguez-Méndez ML, Antonio de Saja J (2012)
73. Sens Actuat B: Chem 166:457–466

74. 62. Ramdani O, Metters JP, Figueiredo-Filho LCS, Fatibello-Filho O, Banks CE (2013) Analyst
75. 138:1053–1059
76. 63. Cai J, Cizak K, Long B, McAferty K, Campbell CG, Allee DR, Vogt BD, La Belle J, Wang J (2009) Sens Actuat B: Chem 137:379–385
77. Yang Y, Chuang M, Lou S, Wang J (2010) Analyst 135:1230–1234
78. Malzahn K, Windmiller JR, Valdes-Ramirez G, Shoning MJ, Wang J (2011) Analyst 136:2912–2917
79. 7. Windmiller JR, Bandodkar AJ, Valdes-Ramirez G, Parkhomovsky S, Martinez AG, Wang J (2012) Chem Commun 48:6794–6796
80. Bandodkar AJ, Molinnus D, Mirza O, Guinovart T, Windmiller JR, Valdés-Ramírez G,Andrade FJ, Schöning MJ, Wang J (2014) Biosens Bioelectron 54:603–609
81. Foster CW, Metters JP, Banks CE (2013) Electroanalysis 25:2275–2282

.

82. C. Hagiopol, J.W. Johnston, Chemistry of modern papermaking: CRC Press; 2011.
83. D. Tobjörk, R. Österbacka, Paper electronics, Advanced Materials, 23(2011) 1935-61.
84. E.W. Nery, L.T. Kubota, Sensing approaches on paper-based devices: a review, Analytical and bioanalytical chemistry, 405(2013) 7573-95.
85. W. Xiao, J. Huang, Immobilization of oligonucleotides onto zirconia-modified filter paper and specific molecular recognition, Langmuir, 27(2011) 12284-8.
86. T.H. Nguyen, A. Fraiwan, S. Choi, Paper-based batteries: A review, Biosensors and Bioelectronics, 54(2014) 640-9.
87. Helland, Åsgeir. "Nanoparticles: a closer look at the risks to human health and the environment perceptions and precautionary measures of industry and regulatory bodies in Europe." (2004).
88. Ratner, Mark A., and Daniel Ratner. *Nanotechnology: A gentle introduction to the next big idea*. Prentice Hall Professional, 2003.
89. Holister, Paul, et al. "Nanoparticles." *Technology White Papers* 3 (2003): 1-11.

90. Wu, Bao-Yan, et al. "Amperometric glucose biosensor based on layer-by-layer assembly of multilayer films composed of chitosan, gold nanoparticles and glucose oxidase modified Pt electrode." *Biosensors and Bioelectronics*22.6 (2007): 838-844.
91. Liu, Hao. *Modified thermal reduction of graphene oxide*. Diss. University of Nottingham, 2014.
92. Gómez-Navarro, Cristina, et al. "Atomic structure of reduced graphene oxide." *Nano letters* 10.4 (2010): 1144-1148
93. Mattevi, C., et al., *Evolution of Electrical, Chemical, and Structural Properties of Transparent and Conducting Chemically Derived Graphene Thin Films.* Advanced Functional Materials, 2009. **19**(16): p. 2577-2583.
94. Erickson, K., et al., *Determination of the Local Chemical Structure of Graphene Oxide and Reduced Graphene Oxide.* Advanced Materials, 2010. **22**(40): p. 4467-4472.
95. Kudin, K.N., et al., *Raman spectra of graphite oxide and functionalized graphene sheets.* Nano Letters, 2008. **8**(1): p. 36-41.
96. Hass, J., W.A. de Heer, and E.H. Conrad, *The growth and morphology of epitaxial multilayer graphene.* Journal of Physics-Condensed Matter, 2008. **20**(32).
97. Wang, X., L.J. Zhi, and K. Mullen, *Transparent, conductive graphene electrodes for dye-sensitized solar cells.* Nano letters, 2008. **8**(1): p. 323-327.
98. Seger, B. and P.V. Kamat, *Electrocatalytically Active Graphene-Platinum Nanocomposites. Role of 2-D Carbon Support in PEM Fuel Cells.* Journal of Physical Chemistry C, 2009. **113**(19): p. 7990-7995.
99. Lu, T., et al., *Electrochemical behaviors of graphene-ZnO and graphene-SnO2 composite films for supercapacitors.* Electrochimica Acta, 2010. **55**(13): p. 4170-4173.
100. Lian, P.C., et al., *Large reversible capacity of high quality graphene sheets as an anode material for lithium-ion batteries.* Electrochimica Acta, 2010. **55**(12): p. 3909-3914.186
101. Magasinski, A., et al., *High-performance lithium-ion anodes using a hierarchical bottom-up approach.* Nature Materials, 2010. **9**(4): p. 353-358.
102. Pan, D.Y., et al., *Li Storage Properties of Disordered Graphene Nanosheets.* Chemistry of Materials, 2009. **21**(14): p. 3136-3142.
103. Park, C.M., et al., *Li-alloy based anode materials for Li secondary batteries.* Chemical Society Reviews, 2010. **39**(8): p. 3115-3141.

104. Lian, P.C., et al., *Large reversible capacity of high quality graphene sheets as an anode material for lithium-ion batteries.* Electrochimica Acta, 2010. **55**(12): p. 3909-3914.186

105. Magasinski, A., et al., *High-performance lithium-ion anodes using a hierarchical bottom-up approach.* Nature Materials, 2010. **9**(4): p. 353-358.

106. Pan, D.Y., et al., *Li Storage Properties of Disordered Graphene Nanosheets.* Chemistry of Materials, 2009. **21**(14): p. 3136-3142.

107. Park, C.M., et al., *Li-alloy based anode materials for Li secondary batteries.* Chemical Society Reviews, 2010. **39**(8): p. 3115-3141.

108. A novel procedure for fabricating flexible screen-printed electrodes with improved electrochemical performance

109. Gurunathan, Sangiliyandi, et al. "Biocompatibility effects of biologically synthesized graphene in primary mouse embryonic fibroblast cells." *Nanoscale research letters* 8.1 (2013): 393.

110. Srivastava, Saurabh, et al. "Electrophoretically deposited reduced graphene oxide platform for food toxin detection." *Nanoscale* 5.7 (2013): 3043-3051.

111. Kumar, Suveen, et al. "Biofunctionalized nanostructured zirconia for biomedical application: a smart approach for oral cancer detection." *Advanced Science* 2.8 (2015).

112. Unnikrishnan, Binesh, Selvakumar Palanisamy, and Shen-Ming Chen. "A simple electrochemical approach to fabricate a glucose biosensor based on graphene–glucose oxidase biocomposite." *Biosensors and Bioelectronics*39.1 (2013): 70-75.